

Thermomechanical Processing of Metal Feedstock for Semisolid Forming: A Review



FRANK CZERWINSKI

Thermomechanical processing of cast structures is an effective solid working route of generating thixotropic morphologies after subsequent partial melting and is in use for decades to manufacture the bulk billet feedstock for thixoforming from a variety of alloys. The solid-state deformation is also critical for coarse particulate feedstock, utilized for semisolid forming either directly or after compaction into billets. Although the original concept, called strain-induced melt activation (SIMA), defined the specific procedure, the term became generally recognized synonym for a variety of thermomechanical treatments offering an opportunity of controlling the solidification microstructure. This review covers transformations during solid-state deformation, reheating to semisolid state and isothermal holding within solidus–liquidus range, and solidification of thixotropic slurries. Essentials of semisolid metal processing, necessary to understand the subject, are supported by details related to specific implementation techniques and alloys. Application examples at laboratory and commercial levels and properties achieved with conventional and severe plastic deformation techniques, for different alloys along with present limitations, are described. The link between solid-state deformation-enhanced melting and liquid metal engineering is emphasized throughout the paper in terms of the common goal of controlling the solidification outcome in order to develop technology for mass-scale production of net-shape components having performance characteristics superior to conventional castings.

<https://doi.org/10.1007/s11663-018-1387-4>

© Her Majesty the Queen in Right of Canada, as represented by the Minister of Natural Resources 2018

I. INTRODUCTION

TO address the needs of modern manufacturing industry, there is a search for a novel technology allowing large-scale production of net-shape components having high-performance characteristics. Although well-established conventional casting like high-pressure die casting, offers vast advantages in terms of manufacturing simplicity, net-shape capabilities, competitive cost and low energy consumption the product quality in terms of its integrity and properties is still not sufficient for some structural applications required in modern transportation vehicles.^[1,2]

When semisolid metal processing (SSP) was invented in the early 1970s,^[3] it generated high expectations and has been seen as a very promising technology with great potentials and capabilities to revolutionize the manufacturing industry. After almost half century of research and despite valuable findings at a laboratory scale, its

global commercialization progress remains rather limited. For a new technology to achieve the commercial acceptance in today's market, clear advantages of competitive cost and superior product properties must be demonstrated. These elements are so far missing and it is emphasized in the literature that semisolid processing has never advanced to become the major metal casting process anticipated by so many early researchers, it requires further development and the critical breakthrough is still expected.

Although the first experiments with semisolid processing involved a product forming from a liquid-state precursor termed as rheocasting, the attention shifted quickly to thixoforming, which on the contrary relies on solid-state precursors. In fact, thixoforming was the first one commercialized and seen as an alternative to complex multistep processes of solid state forming. However, after roughly two decades, rheocasting with then developed a variety techniques of slurry preparations moved again to the center of the research and industrial interest.^[4,5] It is claimed that difficulties with manufacturing of suitable feedstock/billet was the main factor leading to reduced interest in thixoforming despite that it offers broader ranges of design options. There are still limitations on potential alloys used—billet manufacturing process represents an extra step that

FRANK CZERWINSKI is with the CanmetMATERIALS, Natural Resources Canada, Hamilton, Ontario L8P 0A5, Canada. Contact e-mail: Frank.Czerwinski@canada.ca

Manuscript submitted May 11, 2018.

Article published online August 29, 2018.

increases the product cost, and product properties are still lower than those obtained after conventional solid-state forming.^[6–8] To overcome this technology gap, understanding and optimizing the billet manufacturing process are required.

This review covers all aspects of utilizing solid-state deformation preceding melting to manufacture thixotropic feedstocks for semisolid processing in the form of bulk billets and coarse particulates. Along with theoretical fundamentals, necessary to understand the subject, engineering and commercial details of this process are explained. A particular attention is paid to the link between deformation-enhanced melting and the earlier-described liquid metal engineering^[9,10] in terms of their common goal of controlling the solidification outcome to develop technology for mass-scale production of net-shape components having performance characteristics superior to conventional castings.

II. UTILIZING SOLID-STATE DEFORMATION FOR MELTING CONTROL

The solid-state deformation prior to melting offers an opportunity of influencing the solidification outcome through changing the scenario how melting progresses. The treatment of the as-cast microstructure in solid state may involve a single-step or multistep physical processing conducted using a variety of techniques. Its objective is the same as that in the case of liquid metal engineering with a difference that the solidification outcome is affected by manipulating the solid metal prior to its melting rather than the melt itself.

A. Concept Origin

The origin of thermomechanical route of generating thixotropic structures is traced to the invention by Young *et al.*^[11] on a process for preparation of a metal composition suitable for forming in a semisolid condition. As shown in Figure 1, the process comprises of casting, preheating to extrusion, extrusion above the recrystallization temperature (hot working) followed by quenching and subsequent cold working as the second deformation step. At this point of time, the billet is ready to be heated to the semisolid state and subjected to thixoforming. The directional grain structure is obtained by hot extrusion working, being the preferred mode of deformation. According to the invention, cold working may be imposed by upsetting, swaging, drawing, or rolling. The final shaping is performed in semisolid state with a liquid volume fraction from 0.05 to 0.8 (in most cases from 0.15 to 0.5). During heating of a cold-worked structure, recovery and recrystallization occur before liquid formation with the aid of the stored energy. Melting starts preferentially at grain boundaries with a high-energy state, and liquid metal penetrates into high-angle boundaries of recrystallized grains resulting in slurry with solid particles of globular shape. It is believed that the amount and distribution of the stored energy by cold working are the most critical factors in the process since they control the recovery and

recrystallization kinetics as well as the uniformity of the newly formed microstructure. Thus, an assumption of the key role played by the cold deformation substantially limits the effective diameter of the billet manufactured, which is typically of the order of 37 mm (1.5 in.). The technique is generally known as strain- or stress-induced melt activation (SIMA) although the term is not mentioned in the original patent.^[11] The SIMA term was coined by K.P. Young shortly after the patent was issued.

B. Modifications of the Original Concept

Almost a decade later, in 1992, a modified process was patented by Kirkwood *et al.*^[12] The essential difference is a replacement of the hot-deformation followed by cold-deformation sequence (two-step deformation treatment) in Young's invention with just a single step of cold/warm deformation, as shown in Figure 2. Thus, the Kirkwood's method of producing thixotropic material consists of deformation of a fully solidified cast metal below its temperature of recrystallization by cold or warm working using extrusion or rolling. In the next step, the material is heated to semisolid state for thixoforming. In this technique, recrystallization occurs during heating of the billet to thixoforming. The process is known in the literature as recrystallization and partial melting (RAP). An intention of involving warm deformation was likely to increase the penetration depth of deformation and an effective diameter of the billet. However, the *warm* term in the invention^[12] does not bring novelty since deformation in earlier invention^[11] is defined as *cold work* (not room temperature). Technically, therefore, both *cold* and *warm works* define the same deformation at a temperature below the material recrystallization.

As a second major modification, in 1997, Woodhouse^[13] proposed using a single-step deformation as well, but in contrast to Kirkwood's solution, his procedure consisted of hot deformation, as shown in Figure 3. The Woodhouse's invention is also described

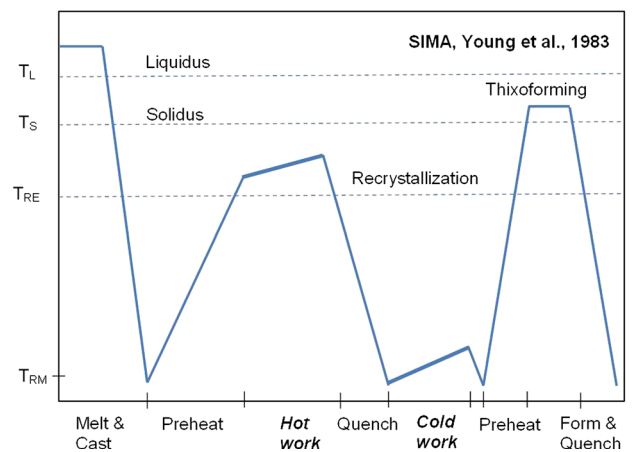


Fig. 1—Time-temperature profile of SIMA solid-state deformation concept for melting control: casting-hot deformation-cold deformation-thixoforming, invented by Young *et al.* Adapted from Ref. [11].

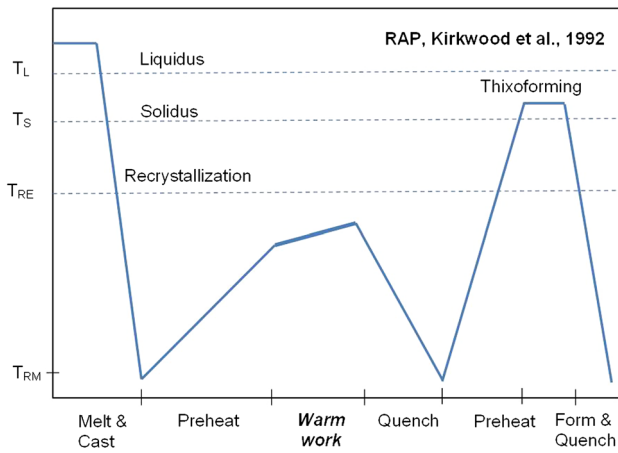


Fig. 2—Time-temperature profile of RAP solid-state deformation concept for melting control: casting-warm/cold deformation-thixoforming, invented by Kirkwood *et al.* Adapted from Ref. [12].

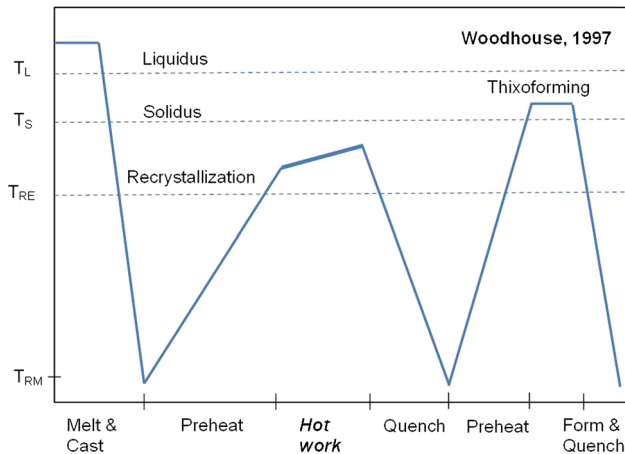


Fig. 3—Time-temperature profile of solid-state deformation concept for melting control: casting-hot deformation-thixoforming, invented by Woodhouse, plot created based on description in Ref. [13].

in Reference 14. To emphasize differences between individual concepts, Figures 1, 2, and 3 were edited for a consistency. Following hot deformation, billet is preheated to semisolid forming. There is no specific name or acronym associated with the Woodhouse's method. The novel element of the Woodhouse's procedure is an elimination of cold/warm deformations, claimed to be the essence of two earlier inventions.^[11,12] In contrast to SIMA and RAP, there is no static recrystallization during heating to semisolid forming. A practical difference between these three deformation scenarios is the achievable effective diameter of the billet. A requirement of sole hot deformation expands substantially the achievable effective diameter of the billet. In summary, these three inventions, covering two-stage hot deformation followed by cold deformation,^[11] a single cold/warm deformation,^[12] and a single hot deformation,^[13] run out all practical possibilities of the temperature window.

Over the subsequent years, a number of treatments based on the concept of melting enhanced by prior deformation were introduced mainly at the laboratory scale. The differences are expressed throughout the type and amount of deformation, temperature, time intervals, and other processing parameters. For example, during fabrication of the AZ91D magnesium billet, the heating rate to temperature of isothermal holding following SIMA was claimed to be essential for obtaining the primary solid particles with a size of 50–60 μm .^[15] The common research trend is a replacement of deformation sequence hot and cold with just a single either hot- or cold-warm stage. As such, they often fall into scenarios already described in previous inventions.^[12,13] Hence, the proposed SIMA modification, through elimination of cold-deformation step and leaving just warm multiforging,^[16] falls into the scenario proposed earlier by Kirkwood *et al.*^[12] Similarly, the essence of the recently published thermo-mechanical treatment, leading to thixotropic structures, called two-step SIMA (TS-SIMA)^[17–19] is omitting the cold-working step of the original SIMA procedure. In practice, the TS-SIMA process follows the deformation option, invented earlier by Woodhouse.^[13] It should be noted that the same term of TS-SIMA was recently introduced for an entirely different method where a single cold deformation is followed by two-step isothermal holding in the semisolid range using a salt bath. Between steps of isothermal holding, the material is quenched to room temperature.^[20,21]

C. Literature Terminology

The terminology used in the literature is inconsistent, which makes it difficult to compare results from different studies and it is anticipated that this review will help to clarify the subject. The SIMA term is used in the literature, almost commonly, as a general term covering deformation-enhanced melting, following not only the two-step deformation treatment as proposed by Young *et al.*^[11] but by a variety of deformation patterns. Accordingly, the processes exploring a single-step uniaxial compression of the Al-Zn-In alloy at room temperature,^[22] a compression of the AZ91D alloy at 230 °C,^[23,24] an equal channel angular extrusion of the AZ91D alloy at 280 °C^[25] or a single hot extrusion of Mg-Gd-Y alloys at temperature of 440 °C,^[26] corresponding to either RAP or Woodhouse's method, are all called in the associated papers as SIMA. This also includes the two-step deformation but with reversed sequence to that described in the original SIMA concept: first the cold-deformation step of rolling, then the hot-deformation step of extrusion.^[27] Moreover, the SIMA term is used for thermo-mechanical treatment of alloys being already in the wrought state.^[28] The same SIMA term is used for generation of spheroidal structures by a deformation at temperatures of semisolid range^[29] or deformation in semisolid state followed by isothermal holding between solidus and liquidus.^[30,31]

The original meanings of terms SIMA and RAP are sometimes mixed and confused as well. For example, SIMA is erroneously portrayed as a single-step deformation and differentiated from RAP through deformation temperature of this single step only, *i.e.*, *hot vs warm* deformation.^[32,33] In turn, the RAP acronym, which does not have a letter referring to deformation, is used to describe just a step of recrystallization followed by melting after any method of previous deformation. Accordingly, the term is seen as a stage within the SIMA process (casting, hot working, cold working and RAP), creating confusion.^[16] To correctly understand the particular thermomechanical process, therefore, its detailed description rather than acronyms and process names should be reviewed.

While during manufacturing of the bulk billet feedstock the solid-state deformation is deliberately imposed, there are examples when the feedstock deformation is a side effect of the feedstock manufacturing process. This is the case for the coarse particulate feedstock, called chips or pellets produced by cutting or other forms of mechanical comminuting of cast ingots.^[34–36] The coarse particulates are used in thixoforming either directly or after a compaction into larger billets.

To describe the solid-state processing, aimed at influencing melting behavior of metals, the term of thermo-mechanical processing is used.^[37,38] In some cases, however, when excluding preheating to thixoforming, the treatment itself may involve just a deformation.

III. GENERATION OF THIXOTROPIC STRUCTURES DURING SEMISOLID PROCESSING

The essence of SSP is a replacement of dendritic structures, prevailing during conventional casting, with nondendritic morphologies.^[39,40] At temperatures of the solidus–liquidus range, slurries with discrete spheroidal solid phase suspended in a liquid matrix were found to exhibit thixotropic behavior with a time- and shear-dependent flow. Thus, after applying shear, solid particles move easily passing one another and flow at solid fractions well exceeding 60 pct.^[41] This is in contrast to dendritic morphologies where the liquid entrapped between dendrite arms gains increased viscosity, blocking alloy flow often at solid fractions of as low as 10 pct.

A. Thixotropy in Metallurgy

Thixotropy is defined as the progressive decrease in viscosity with time for a constant applied shear stress, followed by a gradual recovery when the stress is removed. The phenomenon was discovered in 1923 by Schalek and Szegvari^[42] in nonmetallic systems. During experiments with aqueous iron oxide gels, they revealed that just gentle shaking transformed gel into homogeneous liquid. Such a finding was surprising since at that time, these kinds of physical transformations had only been known to occur by changing temperature when gels would melt on heating and then re-solidify on cooling. The term thixotropy, which originally referred to

reversible changes from fluid to solid-like elastic gel, was introduced by Peterfi in 1927 as a combination of two Greek words: *thixis*: stirring or shaking and *trepo*: turning or changing.^[43] Following this discovery, various systems were studied, including clays, oil suspensions, creams, drilling mud, flour doughs, flour suspensions, fiber greases, jellies, paints, and starch pastes.^[44]

Half a century later, thixotropy found its way into metallurgy when Spencer, Flemings, and co-workers revealed that applying shear during solidification of the Sn-15 pct Pb alloy substantially reduced the stress measured.^[3] In fact, the stress at a given temperature below the liquidus was orders of magnitude less than when the alloy was cooled to that temperature without shear. Decreasing temperature leads to a rapid increase in viscosity, but the higher the shear rate, the lower the maximum viscosity value and the shorter the time to reach its steady state (Figure 4). At the core of the cause of stress reduction is an interaction between solid phase related to morphological changes in semisolid slurry and, in particular, a replacement of dendritic morphologies with spheroidal structures. This finding constitutes a base of SSP, also referred to as semisolid metallurgy.^[45] An example of a suspension of interacting solid particles is shown in Figure 5. For well-separated particles, the viscosity η is described by equation^[46]:

$$\eta = \eta_0 \left(1 - \frac{\Phi}{\Phi_M} \right)^{-2.5\Phi_M}, \quad [1]$$

where Φ is the solid fraction of the suspension and Φ_M is its maximum value at close packing. An increase in viscosity may result from a change in solid fraction or morphology. In case of solid fraction, change is interpreted as an increase in the effective volume fraction Φ_{eff} , which replaces Φ in Eq. [1] and takes into account both the solid and the entrapped liquid.^[47] However, the solid morphology (*e.g.*, dendrite *vs* globule) itself depends on the shear rate.^[48] As a result, for the same solid fraction Φ , different morphologies will

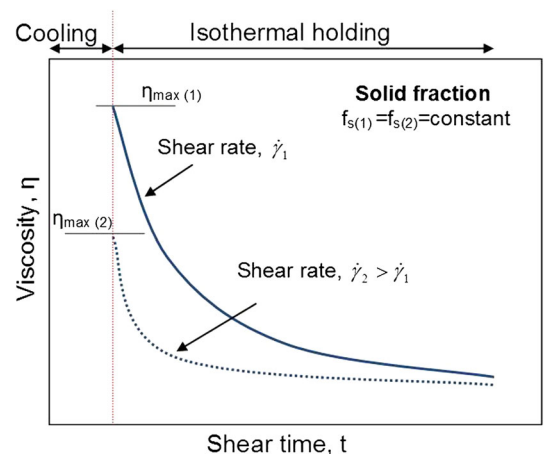


Fig. 4—Influence of the shear rate on the apparent viscosity development. The initial state of alloy for $t = 0$ is fully liquid and cooling conditions are identical in both cases to reach the same temperature of isothermal holding (*i.e.*, the same solid fraction). Reprinted from Ref. [45].

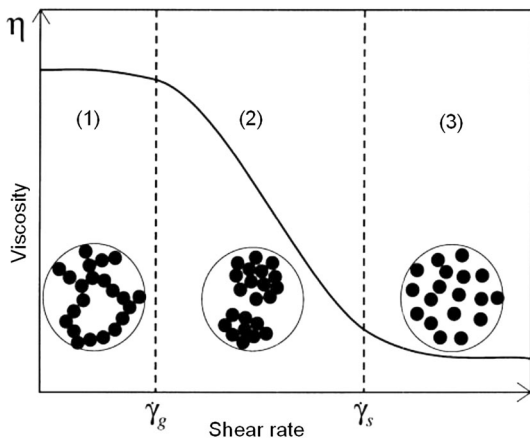


Fig. 5—Morphological changes of thixotropic suspension of interacting particles during shear showing decreases in velocity between the shear rates $\dot{\gamma}_g$ and $\dot{\gamma}_s$: 1. percolating network, 2. dispersed suspension, and 3. suspension of clusters (computer modeling). Reprinted with permission from Ref. [47].

lead to different viscosities. The benefits of SSP are pronounced both in the solidus–liquidus range *via* improved processing behavior and after solidification, through better properties of the solid alloy.

B. Benefits of Thixotropic Slurries

The benefits of nondendritic morphologies at the stage of forming in semisolid stage are pronounced through their flow characteristics. The science of flow and deformation due to movements of matter, describing the relationship between force, deformation and time is called *rheology*. Deformation is the process of changing the relative position of the various parts in a body. To create flow, a stress must be applied. Upon deformation, which changes relative position of particles, spontaneous return to the undeformed shape takes place and is called elasticity. There are irreversible changes leading to dissipation of the mechanical energy as heat. The term rheology originates from a Greek *panta rei*: everything flows and was introduced by Bingham.^[49]

There are four major groups of fluids^[50,51]: (1) time independent or purely viscous fluids (Newtonian and non-Newtonian fluids), (2) time dependent fluids (thixotropic and negative thixotropic fluids), (3) viscoelastic fluids and (4) complex rheological fluids. From the rheological point of view of a perfect matter, three types are distinguished: St. Venant, Hookes, and Newtonian. The liquid iron solution is widely recognized as a Newtonian perfect matter. Newton was the first who assumed that the resistance of the liquid during the flow is proportional to the relative velocity of the particles^[52]:

$$\eta = \frac{\tau}{\dot{\gamma}}, \quad [2]$$

where η is coefficient of viscosity (Pa s), τ is shear stress (Pa) and $\dot{\gamma}$ is shear rate (s^{-1}).

Non-Newtonian and time-independent flow behavior was observed for some liquid metal systems.^[37] A unique property of the flow behavior during semisolid processing is related to the non-Newtonian behavior of an alloy

where due to shear, the particle interconnections will break up, its viscosity will fall leading to a flow like a liquid. After resting for a certain time, globules will connect, increasing the viscosity to the extent such that the alloy is capable of supporting its own weight, as is the case for completely solid phase. The apparent viscosity of slurries is dependent on shear rate and time; the more vigorously they are stirred, the more fluid they become.

Under normal thixoforming conditions, the semisolid slugs experience rapid compression before flowing into the die cavity. It means, within a very short time interval, they experience intense shear thinning with the flow behavior changing from solid-like matter, being capable to support its own shape, to that of a viscous liquid.^[53,54] The technique of semisolid rapid compression is used to assess the semisolid flow behavior through generating load–displacement curves, as it was the case for Al-30Si-5Cu and Al-30Si-5Cu-2Mg* spray-

*All alloy compositions in this report are in wt pct, unless indicated otherwise.

formed alloys.^[55]

C. Rheo-processing Route

To generate a thixotropic structure during rheo-processing, many methods of a liquid metal engineering were developed, in the early days based on various forms of melt agitation such as mechanical, ultrasound or magnetic. During those days, it was thought that one had to shear off and break the dendrites during cooling the liquid down into the two-phase region. Then, novel concepts of generating thixotropic structures from a liquid precursor were introduced where through manipulating the molten metal, the “copious nucleation” was activated capable of producing slurry with the ideal semisolid structure directly from the melt. This includes techniques of swirl enthalpy equilibration, continuous rheo-conversion, sub-liquidus casting, or new rheocasting process among others.^[1,56–58] In addition, there are still efforts to improve effectiveness of mixing concepts by incorporating innovative solutions, *e.g.*, gas-enhanced ultrahigh-shear mixing.^[59] Exploring cavitation and gas bubble dynamics in liquid metals and understanding their high densities at low vapor pressure combined with a large surface tension coefficient creates new opportunities.^[60]

The extensive list of major technologies of liquid metal engineering developed at commercial and laboratory scales is provided in Table I. In this table, magnesium injection molding (thixomolding) is also included, as a universal technology capable of utilizing both the rheo- and thixo-processing routes.^[1] Recent developments indicate that exploring the synergy of melt chemistry and physical treatments achieved through liquid metal engineering allows the creation of the optimal conditions for nucleation and growth during solidification, generating the designed morphologies.^[10] As such, there are still options to improve solidification

Table I. Techniques of Generating Thixotropic Structures Through Liquid Metal Engineering

Process Names	Organizations	Countries	Technique Used to Generate Slurry	Alloys	References
1 slurry-on-demand (SoD) (*)	Mercury Marine	USA	cooling and stirring alloy to nucleate and create a partial solid phase	Al	4
2 Hitachi	Hitachi Metals	Japan	electromagnetic stirring in the shot sleeve	Al	215
3 Honda	Honda	Japan	chilling block with agitating function is inserted into melt	Al, Mg	216
4 semisolid rheocasting (SSR)	Idra Prince	USA/Italy	stirring liquid alloy with a rod mixer	Al	217, 218
5 injection molding (thixomolding)	Dow Chemical Company	USA	melting particulate feedstock in barrel/injection screw system	Mg	218 through 221
6 swirled enthalpy equilibration device (SEED)	Alcan International STAS, Inc.	Canada	extraction of a controlled quantity of enthalpy from the molten metal charge	A356, AA6061	221 through 224
7 Gibbs	Gibbs Die Casting	USA	stirring	Al	225
8 spray casting (Osprey)	OSPREY Metals Ltd., Wales	UK	atomization of the liquid metal	Al	225 through 228
9 induction heating/stirring	CSIR Council for Scientific and Industrial Research	South Africa	stream into droplets conversion of the liquid metal to a semisolid state by stirring with an induced electromagnetic field	A356	229
10 rheo-diecasting (RDC)	Brunel University	UK	dendrite fragmentation with twin screw slurry maker	Al/Mg, AZ91, AM50	230, 231
11 Buhler semisolid metal casting	Buhler	Switzerland	stirring	Al/Mg	232
12 advanced thixotropic metallurgy (ATM)	CSIRO Commonwealth Scientific and Industrial Research Organisation	Australia	pressure waves within runners	Al/Mg	233
13 continuous rheo-conversion (CRP)	ACRC/MPI Advanced Casting Research Center/Metal Processing Institute	USA	reactor provides heat extraction, copious nucleation, and forced convection during the initial stage of solidification, thus leading to globular structures	A383, AM60	234, 235
14 direct thermal method (DTM)	University College Dublin	Ireland	globules achieved <i>via</i> naturally occurring thermal environment	A356	236, 237
15 controlled diffusion solidification	Worcester Polytechnic Institute	USA	two liquid metals of predetermined composition and temperature are mixed producing a globular microstructure	Al/Mg	238
16 new rheocasting (NRC) or UBE process (**)	UBE Industries	Japan	relies on thermal treatment of melt instead of stirring	AZ71	239, 240
17 sub-liquidus casting	THT Presses	USA	pouring grain refined alloy at near-liquidus temperature into die	Al	241
18 self-inoculation method (SIM)	Lanzhou University of Technology	China	addition of self-inoculant to melt, then pouring the melt to a mold through a multistream mixing cooling channel	AM60	242, 243
19 in-ladle direct thermal control (TDC)	Advanced Material Center, Korean Institute of Industrial Technology	Korea	globules are obtained only through thermal control, that is, by in-ladle DTC rheocasting	Al	244

Table I. continued

Process Names	Organizations	Countries	Technique Used to Generate Slurry	Alloys	References
20 chemical grain refinement	Norsk Hydro A.S.	Norway	grain refiner combined with controlled rapid solidification	Mg	245
21 gas-induced semisolid (GISS)	Massachusetts Institute of Technology	USA	mixing by fine gas bubbles injected through a graphite diffuser	AA7075 Al-Zn-In A356	246
22 near-liquidus molding	Husky Injection Molding Systems Ltd.	Canada	tight control temperature within a narrow range around the liquidus	AZ91, AM60	1, 142

(*) Term used also for rheocasting route (a.k.a. "slurry-on-demand" or "SoD"). (**) There are two versions of NRC process: (1) molten alloy is poured directly into a mold and through careful temperature control during cooling a spheroidal semisolid microstructure is achieved and (2) molten alloy is poured onto a cooling slope and then into a mold before processing. The second version is also called *the cooling slope method*.

microstructures. For example, an electric field imposed affects the solidification process. The direct current field of 20 or 200 A/cm², imposed during solidification of the Sn-10Cu alloy, altered the phase-transformation sequence and suppressed the nucleation of the primary ϵ phase.^[61] Moreover, applying direct current during solidification enhanced the grain nucleation and inhibited grain growth. For the Sn-50Pb alloy, the average grain size decreased from 1632 to 567 μm with direct current density of 1.5 A/mm² compared with the case without current-related enhancement.^[62]

It should be noted that there is research showing that partial melting of as-cast structures followed by some form of isothermal holding may lead to elimination of dendritic morphology. For example, semisolid metal forming process for converting a dendritic microstructure of a hypoeutectic aluminum silicon alloy A357 into globular forms by slow heating at a rate of 20 to 30 °C/min to semisolid state and maintaining at the solidus–liquidus range until globules are formed.^[63] Another example is the controlled slow heating to a temperature between solidus and liquidus followed by an isothermal holding process that had a positive effect on solid particle spheroidization of the as-cast Al-5.8Cu alloy.^[64] Similarly for the A356 and A357 alloys heating to 588 °C at 278 °C/min and holding for up to 3 minutes followed by quenching led to globules with a diameter of 120 μm . It is interesting that heating rate for the same alloys in both studies differ by tenfold. Also isothermal holding of 3 minutes is relatively short to cause drastic diffusion-controlled changes. In both cases, however, hypoeutectic alloys contained solid Si particles (in solidus/liquidus range), so the particles are the key factor contributing to changes during melting. It is suspected that the silicon particles with a diameter of 5 μm acted as nuclei for globules growth.^[65] Similar experiments were reported for the AM60B magnesium alloy with grains refined by MgCO₃.^[66] It was found that small and spheroidal primary particles can be obtained after partial melting of alloy having a grain size of 69 μm .

The role of cooling rate is clearly shown in other experiments where a variety of the as-cast structures of the AlSi7Mg alloy with a grain size ranging from 1.4 mm to 160 μm were obtained by controlling solidification conditions.^[67] After partial melting and isothermal holding at 580 °C, fine-grained structures evolved into well-rounded globules after 5 to 10 minutes. In particular, structures with medium-sized dendrites evolved to globular morphologies with a relatively large particle size after a long isothermal holding time, while coarse-grained dendritic structures were not able to evolve to globular morphologies at all. In another experiment with the ZA27 zinc alloy, small rods with a diameter of 45 μm developed globular morphologies after heating for 90 minutes at a temperature of 475 °C.^[68] There are zinc alloys Zn-Al_x-Cu_y, Zamak, tested with thixoforming, where liquid metal treatment was used instead of solid-phase deformation.^[69]

At the same time, there are numerous examples proving that direct melting of the as-cast dendritic structures did not lead to globular morphologies.^[36,70]

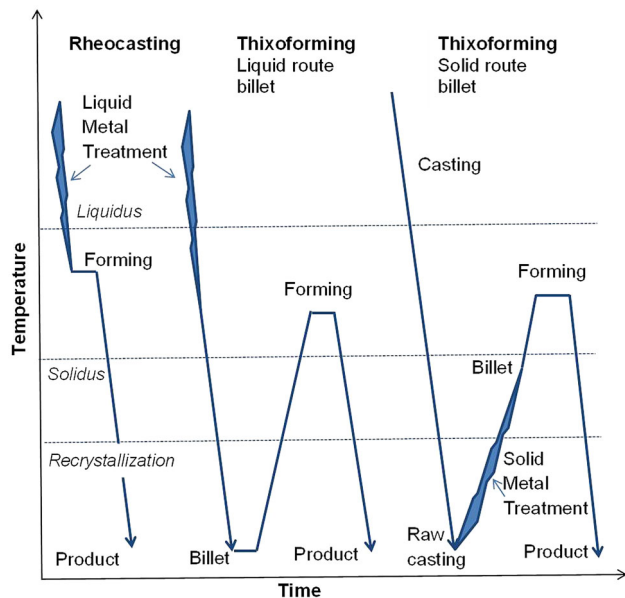


Fig. 6—Schematic diagram of temperature–time explaining concepts of rheocasting and thixoforming based on billet manufactured by liquid route and solid route.

D. Thixo-processing Route

Thixoforming is a general term used to describe the near net-shape forming from a partially melted nondendritic billet within a metal die (Figure 6). In case the component shaping is performed in a closed die, it is called thixocasting. When the shaping process takes place in an open die, it is called thixoforging. An advantage of the thixo-route is that forming is free from handling the superheated liquid metal. Thixoforming is used by a number of industries producing aluminum and magnesium alloy parts.^[1,38] Some progress was achieved in its application to high-melting-point metal alloys.^[71–73] There are also disadvantages of thixoforming, and the most frequently cited of these include high cost of the feedstock material compared with normal foundry alloys, scrap generation since billets are supplied in specific lengths, no possibility for scrap produced to be recycled on site, alloy degradation, and loss during the stages of preheating to semisolid state and alloy surface oxidation. In the case of magnesium alloys, the latter requires protective atmospheres to inhibit reactions with oxygen.^[74–76] Moreover, a capital investment is needed for multiple induction-heating systems, there is a limitation on potential alloys used, and the feedstock microstructure deteriorates during partial melting prior to forming.

E. Billet Manufacturing for Thixoforming

The billet precursor for thixo-processing is manufactured either by liquid-state casting where in principle all liquid metal engineering routes can be utilized or by solid-state processing (Figure 7). For commercial

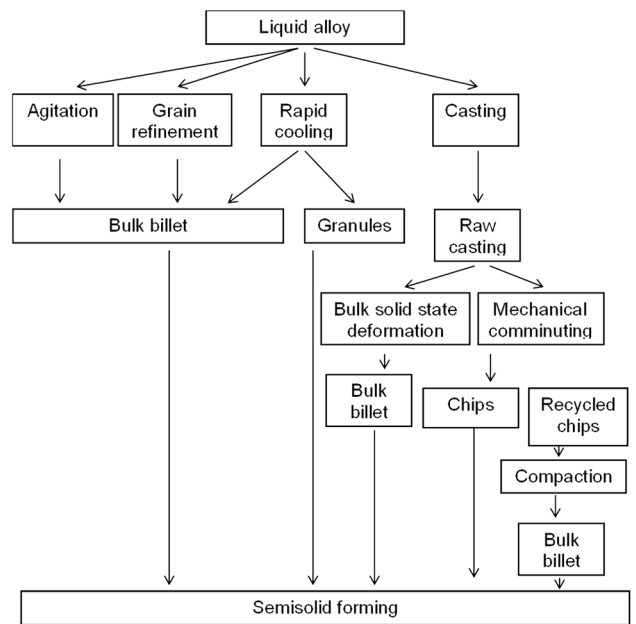


Fig. 7—Schematics of techniques available for manufacturing billets for thixoforming.

purposes, continuous casting is preferred. The new process is capable of continuous semisolid casting of billets of aluminum alloys with a diameter of 70 to 150 mm by agitating the alloy in the flow vessel applying a mechanical screw and an electromagnetic stirrer.^[77] The microstructure generated consisted of predominantly globular particles with fine eutectics excluding a 2-mm surface region being dendritic. In a similar technique, the continuous casting cell with the electromagnetic stirring of 10 Hz frequency was used to manufacture billets of the Al-6Si-2Mg alloy.^[78] The system consisting of melting furnace, melt duct, ceramic filter, graphite cooler, electromagnetic stirring device, water cooling and billet-withdrawal machine was delivering billets at the speed of 2 to 5 mm/s.

A different approach in billet fabrication through casting route is based on cooling control during solidification to avoid extensive dendrite growth.^[79] The method does not produce billet with globular morphologies but rather with very fine dendrites. Then, after reheating the fine dendrites transform to globular forms. The principle is based on spray forming, which converts molten alloy directly into a semifinished product, *e.g.*, Osprey's process.^[80] In this technique, the property benefits arise from rapid solidification, which promotes microstructural refinement and eliminates macrosegregation. The similar transformation of dendrites into globules was revealed during melting of rapidly solidified granules^[81] (Figure 8). The rapid solidification is also explored through billet manufacturing called rapid slug cooling technology (RSCT), developed at RWTH Aachen, Germany.^[82,83] The RSCT method was tested with both the magnesium and aluminum alloys.

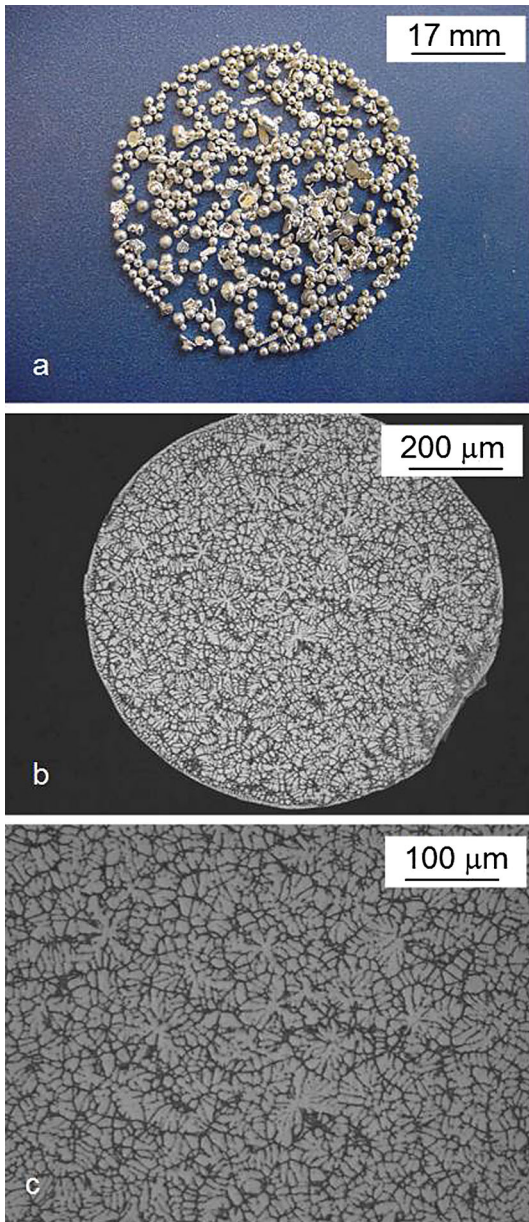


Fig. 8—Granules manufactured of an aluminum alloy by rapid solidification: (a) general view; (b) cross section after etching revealing internal structure of fine dendrites; (c) magnified view of granule microstructure. Reprinted from Ref. [253].

IV. IMPLEMENTING SOLID-STATE DEFORMATION FOR BILLET MANUFACTURING

The essential part of all techniques of manipulating cast microstructure to influence its transformation to globular morphologies during partial melting is the solid-state deformation. With the temperature-processing window defined by key inventions,^[11–13] the focus during the recent decades has been on deformation-implementation methods. When designing the billet manufacturing through SIMA techniques, a number of questions arise. Why so many different deformation

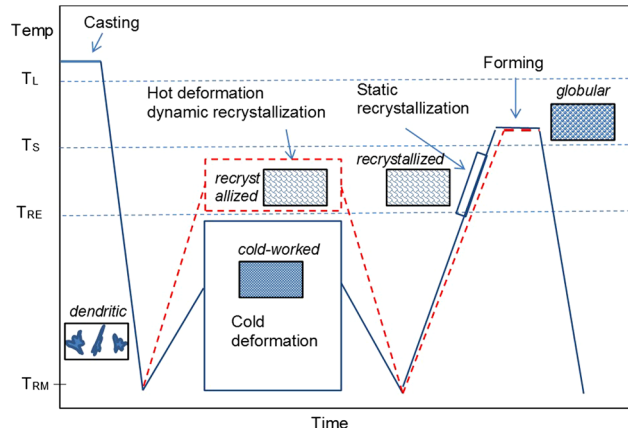


Fig. 9—Schematics of transformations required to convert the as-cast dendritic structure into globular by solid-state deformation followed by partial melting and semisolid forming.

techniques, including exotic ones, are involved in billet preparation? Is it to obtain the larger volume of deformed material or to generate more optimal deformation microstructure? Then, what is the optimal deformation-enhanced microstructure for formation of thixotropic morphologies after partial melting? It is the prevailing wisdom that a deformation (either cold or hot) sufficient to trigger recrystallization (either static or dynamic) is the essential requirement for successful dendrite to globule transition during melting. The required deformation outcome is the equiaxed microstructure at the beginning of melting (Figure 9).

Methods exploring solid-state deformation prior to melting and solidification have some limitations in terms of billet sizes due to the requirement of high and uniform deformation over the whole cross-sectional area. However, they generate high-quality feedstock for thixoforming with a processing potential for alloys designed for wrought processing and high-melting temperature alloys such as steel and superalloys. As explained in this section, deformation processing allows controlling transformations during subsequent melting and represents, in general, an effective approach to the synthesis of materials with desired specific properties. At the same time, the solid-state deformation and recrystallization of conventionally cast dendritic materials by thermomechanical treatments are energy and processing intensive, raising its cost by approximately 3 to 5 times higher than billets manufactured using the magnetohydrodynamic (MHD) stirring process.^[84]

An alternative route of bulk billet manufacturing explores the solid-state compaction of coarse particulates (chips). The particulates may be deliberately manufactured by comminuting cast ingots or generated as a side effect of another process, *e.g.*, part machining. In case of particulates generated during part machining, this route offers an effective way of metal recycling.^[85–88] In fact, individual particulates represent “mini-billets” with their volume getting heavily deformed in the course of manufacturing.

A. Cold Working, Static Recovery, and Recrystallization

Cold working (also called work-hardening) is the plastic deformation of metals below the recrystallization temperature.^[89] The low deformation temperature, typically below 0.3 to 0.5 of the melting temperature, does not allow atoms to rearrange themselves. Cold working introduces defects in the material such as point defects and dislocations, which can store up to 10 pct of the energy of plastic deformation. During cold deformation, the dislocations can initially move through the metal structure but their movement becomes more difficult when new dislocations are generated in due course and their density increases. As a result, dislocations will interact with each other and become pinned or tangled. Cold deformation increases the material strength. The general view and subtle details of internal structure after cold work are shown in Figure 10. At higher magnifications, multiply twins are revealed, having different orientations within each grain with contrast indicating stress concentration at the twin interfaces. The intermetallic compound is distributed along the matrix grain boundary.

When cold-worked metal is subjected to heating, changes take place within cold-deformed structure where new grains are generated by nucleation and growth (Figure 11).^[90] Recovery is a process that starts at low temperatures leading to the decrease of the

density with redistribution of mainly point defects (vacancies and interstitials). Also, dislocations of opposite signs annihilate each other, and dislocations align to form low-energy configurations as is the case in tilt and twist boundaries. During recovery, accumulated strain is relieved to some extent by microstructural and submicroscopic rearrangements, but grains are not entirely strain free. The overall energy released at this stage is rather low. Processes of recovery and recrystallization involve diffusion and therefore depend on thermal activation to cause rearrangement of dislocations and grain boundaries.

The stored strain energy in a deformed material is also the driving force for recrystallization expressed through nucleation and growth of the stress-free grains. Static recrystallization is a phenomenon in which new dislocation-free grains appear in strain-hardened metals and alloys during annealing. For recrystallization to take place, a minimum of cold working is needed; if the deformation is very low, recrystallization does not occur. The recrystallization behaviors are affected by amount of prior deformation, temperature, time, initial grain size, composition and the progress of recovery before an onset of recrystallization.^[89] The process described is sometimes called as discontinuous static recrystallization. In case of deformed materials containing dispersed precipitates, the new microstructure

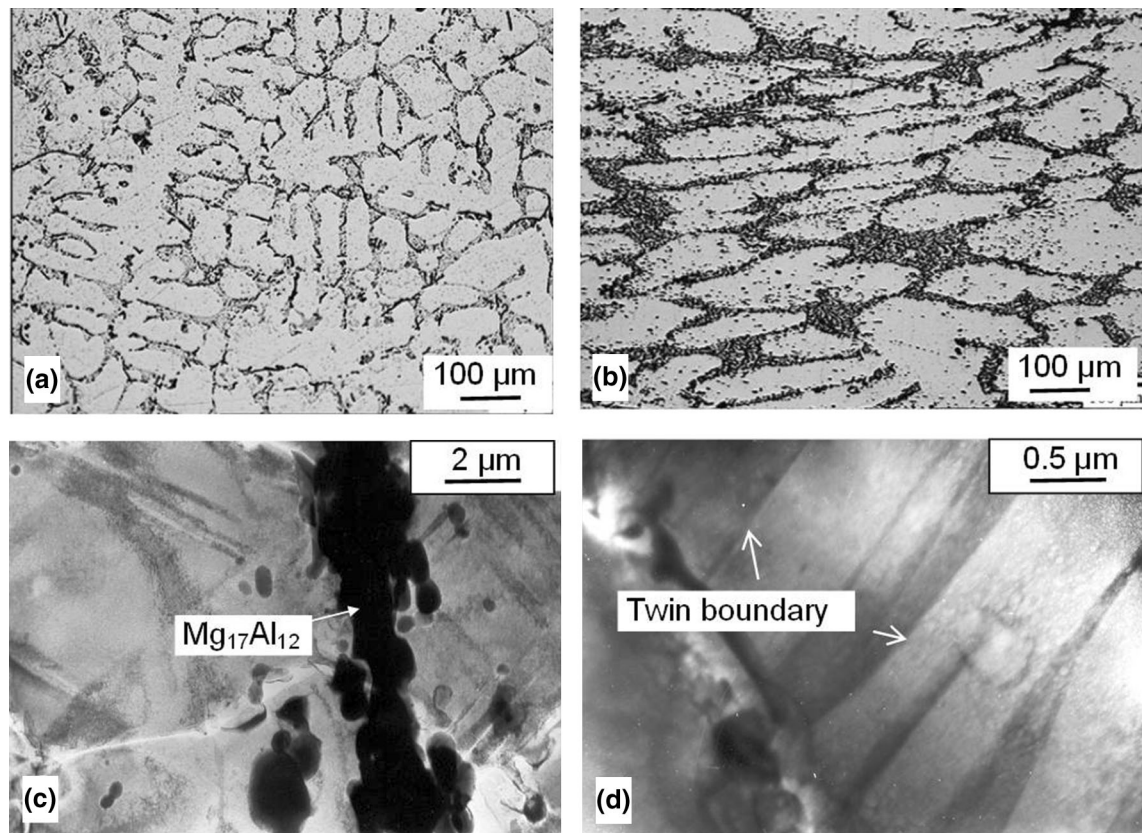


Fig. 10—Deformation microstructures: optical images of A356.2 alloy (a) as-cast and (b) deformed by cross wedge rolling at 225 °C. Reprinted with permission from Ref. [155]; TEM images of an internal structure of grains in Mg-8Al-2Zn alloy cold deformed by extrusion: (c) intermetallic compounds $Mg_{17}Al_{12}$ located at grain boundary; (d) deformation twins inside the α -Mg grain. Reprinted with permission from Ref. [35].

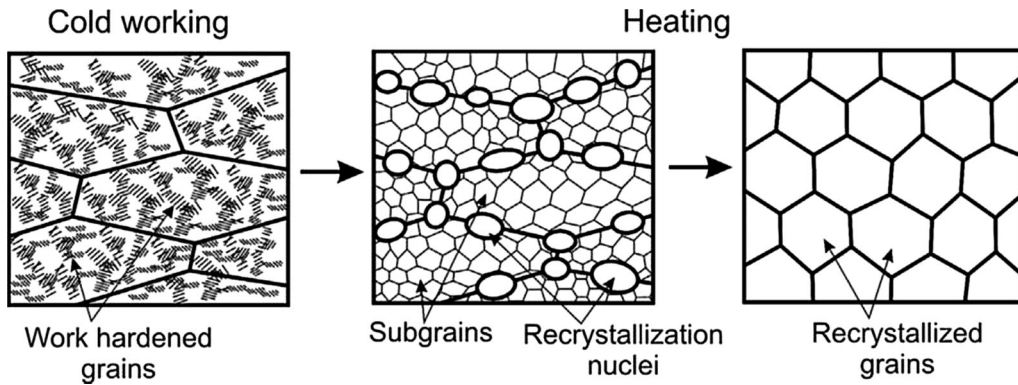


Fig. 11—Schematic representation of the discontinuous static recrystallization taking place during the annealing of strain-hardened materials. Reprinted with permission from Ref. [94].

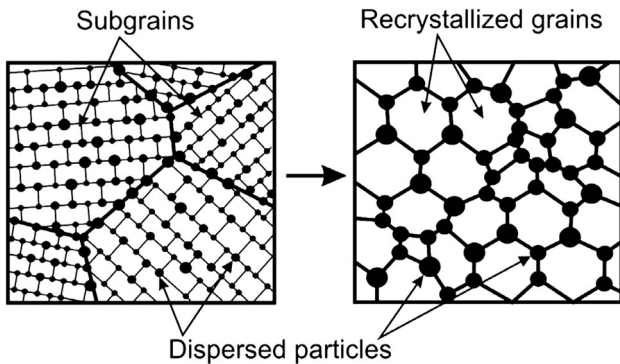


Fig. 12—Schematic representation of the continuous static recrystallization controlled by particle coarsening. Reprinted from Ref. [254].

develops uniformly within the material volume as shown in Figure 12. This process is called *continuous static recrystallization*. The new grains develop by gradual growth of subgrains along with coarsening of particles.^[91] An example of solid-state transformation of the cold-extruded Mg8Al2Zn alloy during heating up to solidus temperature is shown in Figure 13. A significant rebuilding of grains, occurring at 200 °C, suggests recrystallization, and then at 300 °C, banding is seen as a result of chemical segregation. The banding disappears during further heating, and at 460 °C, grain growth occurs. At 480 °C, the solidus temperature is exceeded, and melting starts at grain boundaries.

B. Hot Working, Dynamic Recovery, and Recrystallization

When a metal is worked above its recrystallization temperature, called hot working, the dislocations can rearrange and little strengthening is achieved. The microstructure and mechanical properties formed during hot forming are controlled by work hardening, dynamic recovery, and dynamic recrystallization. Dynamic recovery is the sole softening mechanism in metals where climb and cross slip of dislocations are

easily found as in aluminum, α -Fe, or most BCC metals with high stacking-fault energy (stacking faults in crystalline structures are planar-type defects).^[89,92]

By contrast to static recrystallization, during dynamic recrystallization, new grains form during deformation, without the application of an annealing treatment. At a microstructural level, dynamic recrystallization begins when strain hardening and a process of recovery can no longer store accumulated immobile dislocations. As a result of dynamic recrystallization, some crystal defects are eliminated, such as part of dislocations formed due to work hardening, thus improving hot plasticity and reducing the deformation resistance.^[93] The process also refines microstructure and modifies the crystallographic texture as shown in Figure 14 for the AA1421 aluminum alloy deformed at 400 °C.

During the conventional discontinuous dynamic recrystallization that takes place at elevated temperatures, the new grains evolve by nucleation and growth in materials with low-to-medium stacking-fault energies. Severe plastic deformation can produce new ultrafine grains in any material irrespective of the stacking-fault energy at relatively low temperatures.^[94] This is caused by the gradual transformation of the dislocation subboundaries produced at low strains into ultrafine grains with high-angle boundaries at large strains. This process is termed *in situ* or *continuous dynamic recrystallization*. High stacking-fault energy metals undergo continuous dynamic recrystallization rather than discontinuous dynamic recrystallization during high-temperature deformation.

The commercial alloys used for billets generally have multiphase structure with dendritic morphologies. Thus, hot working will include bending and breaking of dendrites in addition to matrix deformation. For example, during SIMA process of preparing semisolid billet of the ZCuSn10 (88.25Cu, 10.48Sn) alloy that included rolling at 450 °C, the main mechanism was deformation of dendrites.^[95] During subsequent heating, such a structure above solidus the liquid phase filled sharp corners of solid particles with Sn element diffusing from liquid phase into α solid phase.

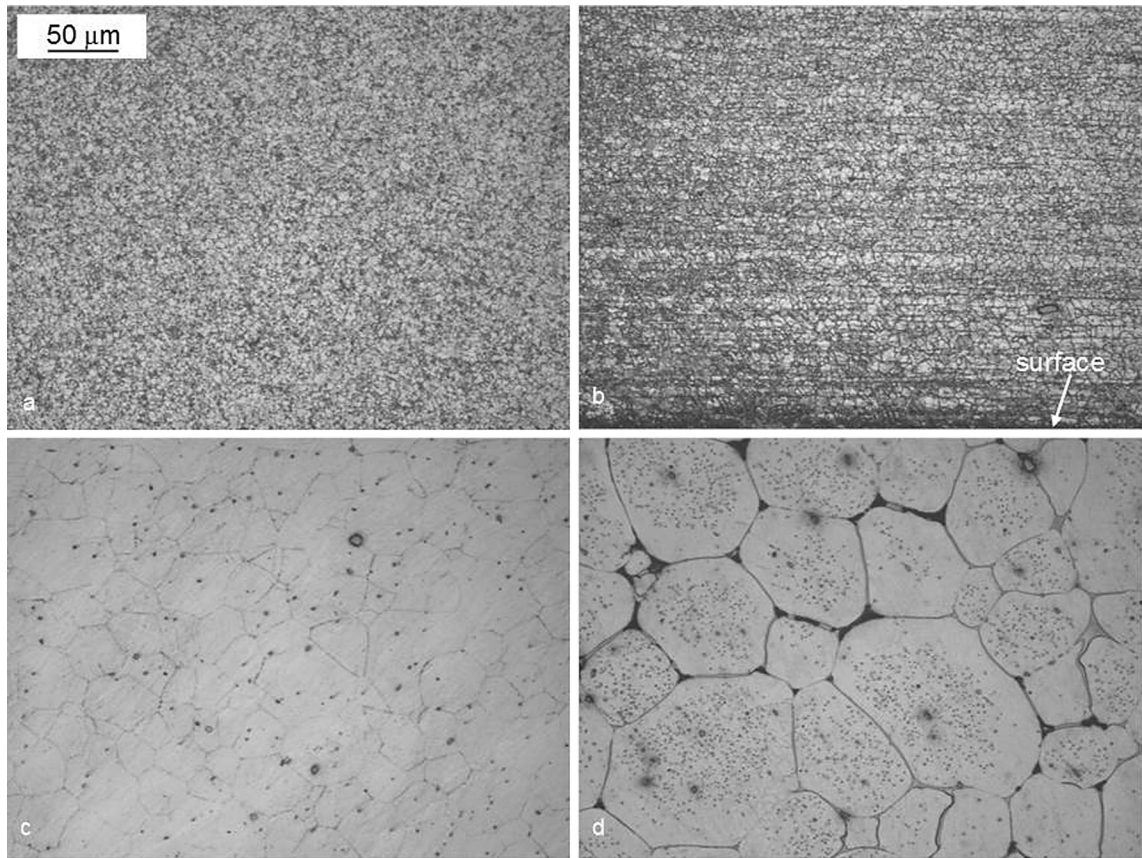


Fig. 13—Microstructure evolution of cold-extruded Mg-8Al-2Zn alloy during heating to solidus range: (a) 200 °C; (b) 330 °C; (c) 460 °C; (d) 480 °C. Holding time of 15 min. The extrusion direction is oriented horizontally. Reprinted with permission from Ref. [35].

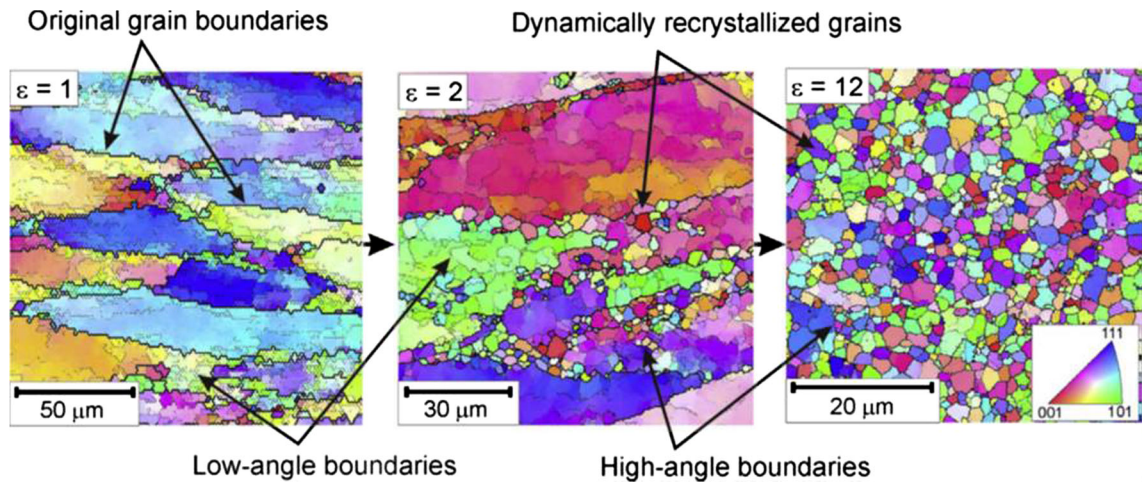


Fig. 14—Development of new grains due to continuous dynamic recrystallization observed by orientation imaging microscopy. The AA1421 aluminum alloy was processed by ECAP repeatedly to a strain of 12 at 400 °C. Reprinted with permission from Ref. [94].

C. Grain Growth During Heating

Grain growth is the process of increasing the average grain size in polycrystalline materials through growing some grains at the expense of shrinking smaller ones.^[96–98] In contrast to recovery

and recrystallization, grain growth is not in direct response to deformation, but it is a thermally driven restoration process that results in lower surface energy of individual grains. In polycrystalline materials, interfaces are unstable, and if

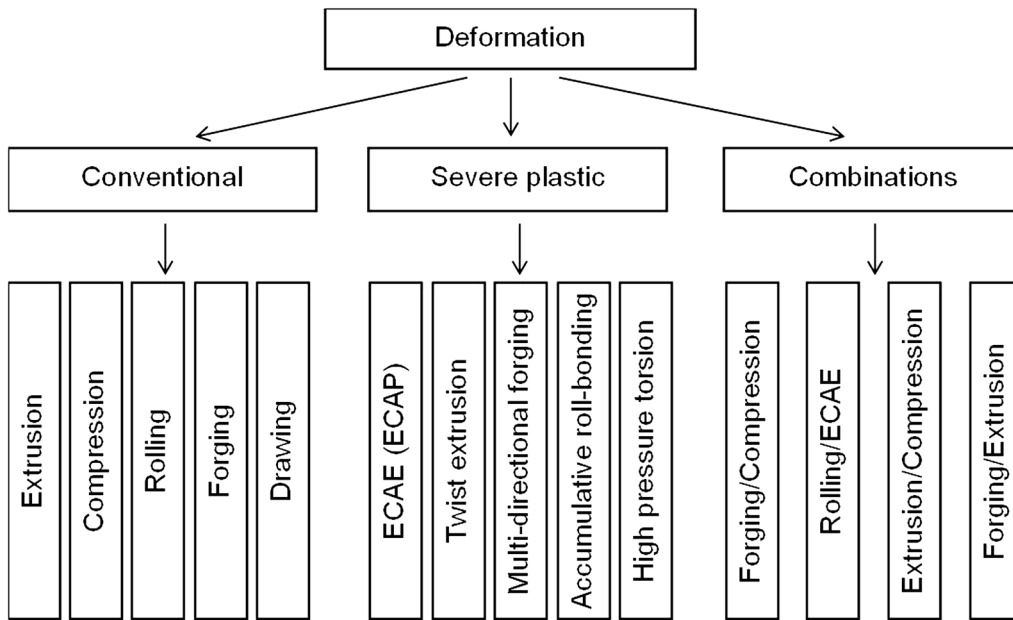


Fig. 15—Schematics of deformation techniques and their combination explored for manufacturing billets for thixoforming.

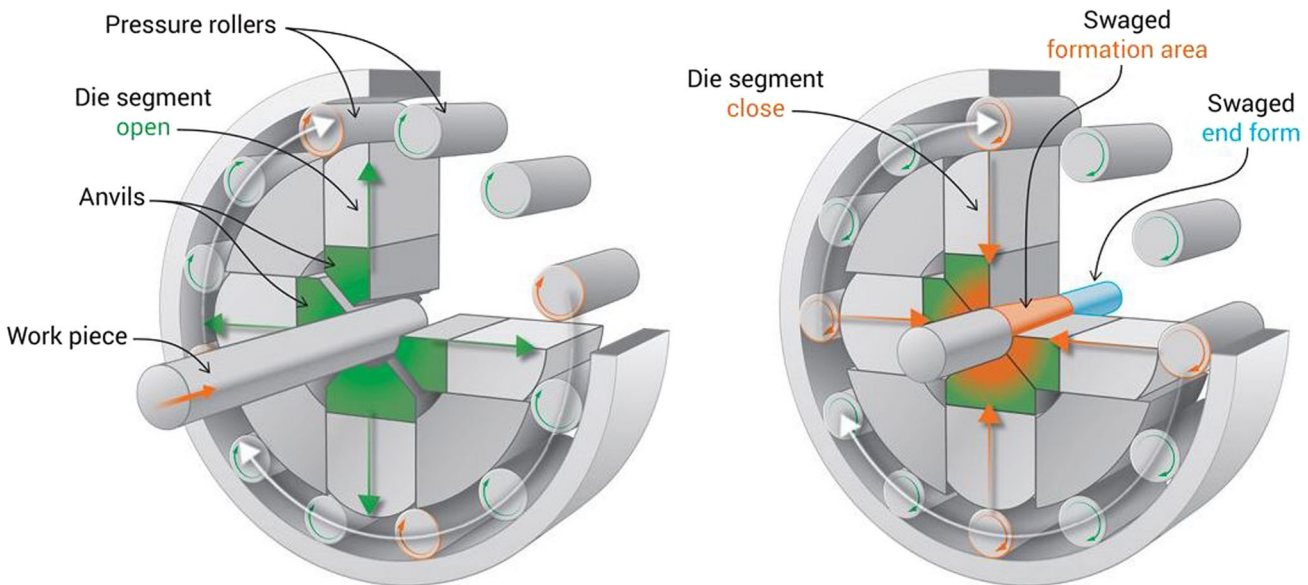


Fig. 16—Metal swaging or radial forging involves the forging of a work piece by use of die that exerts compressive forces by impacts that act around the work circumference. Reprinted from Ref. [101].

atoms have sufficient mobility, they would rearrange to configurations minimizing the total interface energy.

The above processes define the driving force for grain growth. Grain growth may be inhibited through a presence of fine precipitates, restricting the grain boundary movement. The grain growth kinetics is of importance in terms of its relation with the size of globular morphologies in semisolid slurry. Since the globule diameter at the beginning of melting is equal to the size of solid grain at this time, it is beneficial to retard the grain growth.^[35]

D. Deformation Techniques

There is a long list of potential techniques applicable to impose strain to cast structures for the purpose of influencing their subsequent melting. In general, they may be divided into conventional deformation techniques, severe plastic deformation, and their combinations (Figure 15).

1. Conventional deformation techniques

The conventional deformation methods, applicable to billet manufacturing, include rolling, extrusion, compression, drawing or forging. It should be noted that the primary objective here is to impose deformation rather

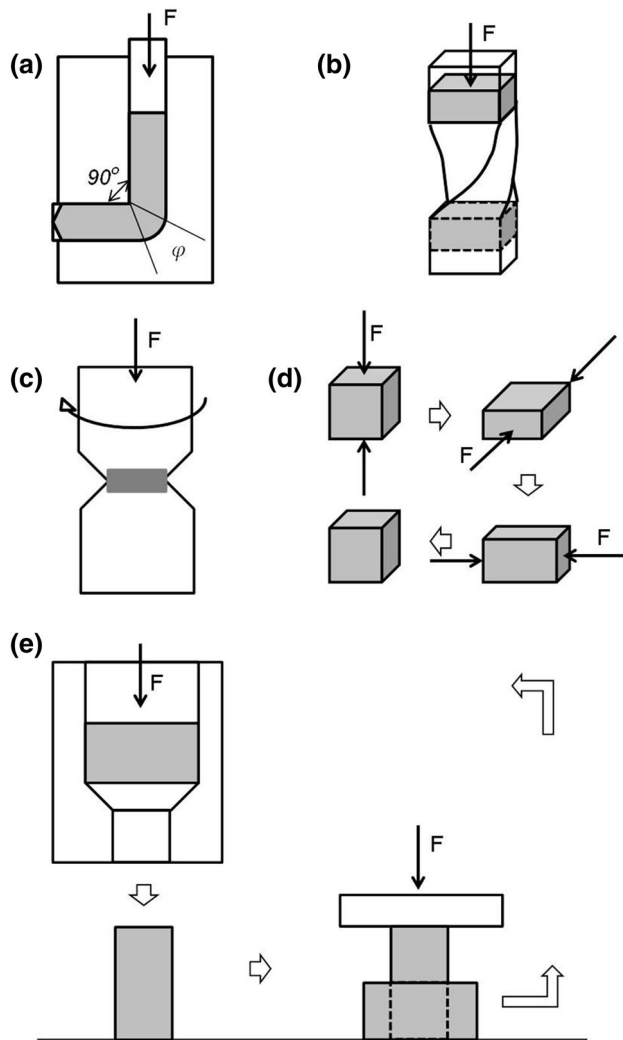


Fig. 17—Principles of selected methods of severe plastic deformation: (a) equal channel angular pressing/extrusion (ECAE), (b) twist extrusion (TE), (c) high-pressure torsion (HPT), (d) multidirectional forging (MDF) and (e) repetitive extrusion upsetting (RUE).

than to create the specific geometric form of a final component. There is a difference in deformation scenarios and amount of strain induced into material during each processing.

Extrusion is the most frequent deformation technique used for a variety of alloys to prepare billets for thixoforming. During extrusion, a block of metal (billet) is forced to flow by compression through the die opening of a smaller cross-sectional area than that of the original billet. The homogeneous deformation during extrusion is favored by (1) low container friction, (2) well-lubricated billet, (3) hydrostatic extrusion condition and (4) indirect extrusion process.^[99] The deformation is more uniform until close to the die entrance where metal flow is restricted. The temperature increase during extrusion is affected by extrusion velocity, extrusion ratio, die preheat temperature, and percentage reduction in area.^[100] Aluminum is the most common hot-extruded material, with billet temperatures ranging from 300 °C to 600 °C. In the extrusion of copper alloys and steels, spontaneous

recrystallization usually takes place during the deformation as the extrusion temperature is well above the recrystallization temperature. *Compression* is a convenient deformation technique during laboratory small-scale experiments. The tensile/compression testing frames or simple hydraulic presses can impose sufficient deformation to small samples. During *rolling*, the work material is plastically deformed by compressive forces between two constantly spinning rolls. As a result, the geometric shape of the work is changed but its volume remains constant. The plastic deformation of the material occurs in the roll zone. Cold rolling is useful for imparting strength and favorable grain orientation. *Metal swaging* or *radial forging* involves the forging of a work piece by use of die that exert compressive forces by impacts that act around the work circumference.^[101] In this process, the work material is not completely restricted by the die and may receive several forging blows per second (Figure 16). These forging strokes are performed by synchronized rollers that act in a cage, which rotates around the part, and the rollers, in turn, enact the motion of the die. Metal swaging is typically performed as a cold-working process.

2. Severe plastic deformation

In addition to conventional processes, there are also techniques of severe plastic deformation, capable of imposing ultrahigh strain into material. The most important deformation methods applicable for billet manufacturing at experimental level include:

- Equal channel angular extrusion (pressing) (ECAE/ECAP),
- Twist extrusion (TE),
- High-pressure torsion (HPT),
- Multidirectional forging (MDF),
- Repetitive upsetting and extrusion (RUE).

The *ECAE*, developed in 1970s, also known as equal-channel angular pressing (ECAP), is a processing method in which a metal is subjected to an intense plastic straining through simple shear without any accompanying change in the cross-sectional dimensions of the workpiece.^[102,103] As shown in Figure 17(a), the workpiece is extruded through a die containing two identical cross-sectional channels, intersecting at an angle ϕ (generally 90 deg or 120 deg). The unique feature of ECAE is the ability to impose a significant cold work without reduction in the cross-sectional area of the deformed material. When conventional deformation processes like rolling, forging, extrusion, and drawing, introduce strain by reduction in the cross-sectional area, in ECAE this objective is accomplished without reducing the part dimensions.^[104]

During *TE*, the material is extruded through a complex designed die, where entry and exit cross sections are identical, but turned for a specific angle β (usually $\beta = 90$ deg).^[105] It causes intensive grain refinement, homogenization and mixing. Since the die has large stiffness and complex design, it provides high hydrostatic pressures and simple shear deformations (Figure 17(b)). In contrast to ECAE, there are two main shear layers perpendicular to the material axis.

HPT relies on applying an additional hydrostatic compression stress on high torsional shearing stress.^[106,107] It is traced back to the work of Bridgman who showed that fracture strain could be increased by applying hydrostatic pressure during a torsion test.^[108] In free torsion, the geometrical changes are usually very small. As a result of combining of those two stresses, fracture strain can be further enhanced and can be increased to infinity at very high hydrostatic compression stresses (Figure 17(c)).

MDF was developed in the early 1990s, as a simple method for applying large strains that is particularly useful for the processing of bulk products.^[109] As shown in Figure 17(d), a prismatic specimen is compressed sequentially along its three principal axes. The shape of the specimen does not change substantially as a result of multiple deformations until the strain in each forging pass is well below 1.

RUE is ultrahigh straining process based on the combination of conventional direct extrusion followed by upsetting of an extruded material in several cycles of severe plastic deformation.^[110] The process begins with the extrusion in order to elongate the grains (Figure 17(e)). After extrusion, the specimen is upset until the initial diameter is reached again, so the direct extrusion process can be repeated. During extrusion and upsetting processes, the grains are fragmented along shearing planes.

As expected, the temperature of severe plastic deformation affects the recrystallized grain sizes as shown during modeling on aluminum (Figure 18). In case of the Mg-Zn-Y-Zr alloy, deformed through a single pass

ECAE at 200 °C the recrystallized grain structure was much finer than those deformed under identical conditions at 400 °C.^[111] Due to HCP crystallography of magnesium, the billet orientation exerted effect on the yield strength and ductility of the deformed alloy. In particular, at a given ECAE temperature, turning the billet orientation 90 deg may lead to an increase in yield strength and a decrease in elongation, or a decrease in yield strength and an increase in elongation.

For the Al-Zn-Mg alloy, after four passes of ECAP, precipitates of 120 nm, the η' , η , T, and E phases were fragmented into groups of fine spherical particles having average sizes of 60 nm.^[112] After eight ECAP passes, the number of these precipitates was increased and their average size reached 65 nm. After post-ECAP annealing at 120 °C and 200 °C for 20 hours, precipitates with larger sizes were aligned primarily along grain boundaries, and finer particles were evenly distributed within grains. Increasing the number of ECAP passes from 4 to 8 led to an increase in the volume fraction of the finer precipitates in the ECAP-processed and -annealed alloy.

To increase strain, two or more different techniques may be combined, and there are many evidences supporting fact that a combination of different techniques is effective.^[113] A schematic, detailing development of internal grain structure during a combination of cold working followed by hot working, is shown in Figure 19. Thus, the initial cold work introduces a high density of dislocations, which transform into polygonized subgrains upon heating to the processing temperature. Then, hot deformation causes subgrain rotation followed by their transformation.

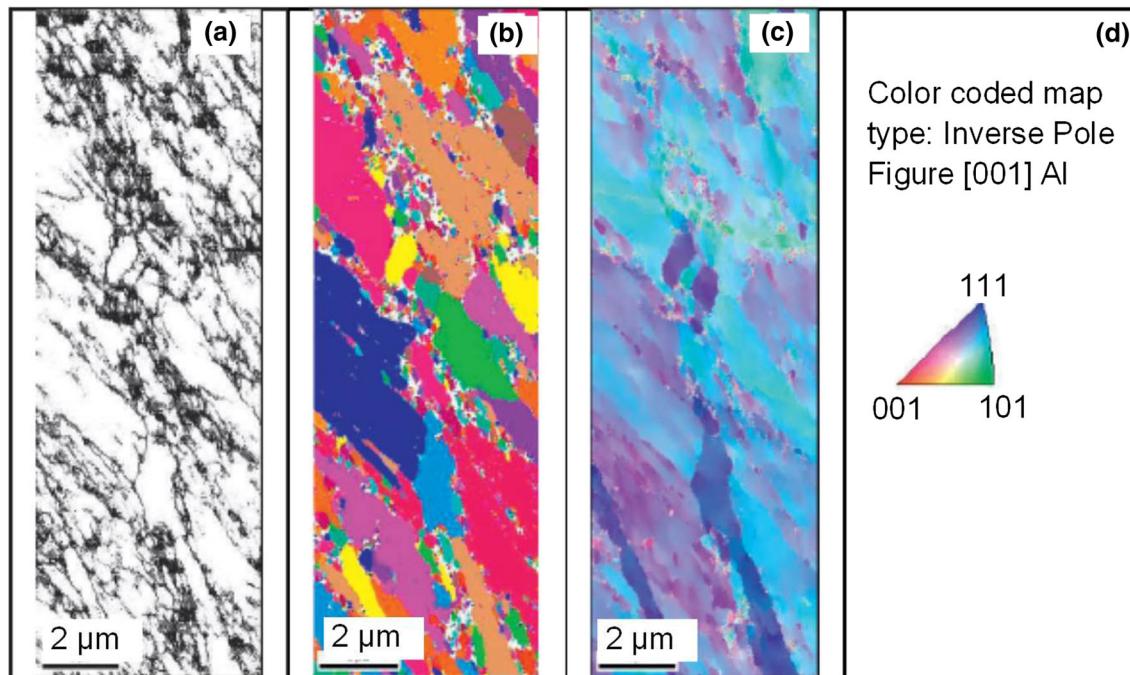


Fig. 18—Modeling of a process of producing ultrafine grains in bulk metallic materials by means of severe plastic deformation using ECAP: (a) the boundaries map; (b) orientation imaging microscopy; (c) inverse pole figure obtained from the transverse section of the sample after four-pass ECAP at 200 °C; (d) standard stereographic projection. Reprinted with permission from Ref. [255].

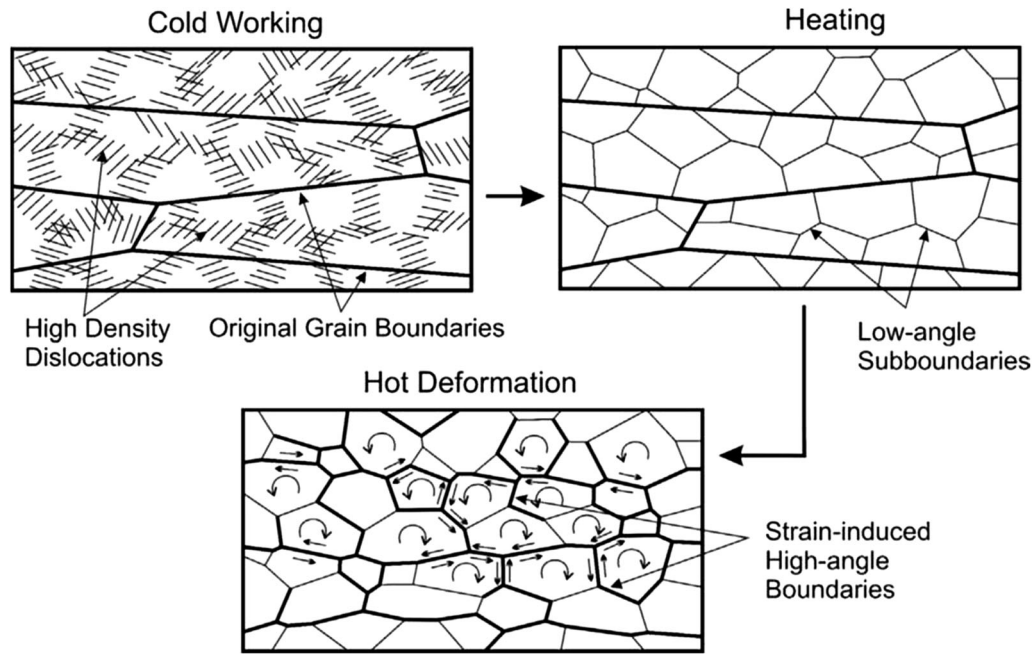


Fig. 19—Schematic illustration of ultrafine grain development during hot deformation of prior cold- and warm-worked alloys. The subgrain rotations taking place are accompanied by sliding along the grain boundaries during hot deformation at low strain rates. Reprinted with permission from Ref. [256].

The assessment of deformation techniques used in billet processing comes often from solid-state property after deformation, not necessarily after semisolid processing. At this stage, the severity of deformation and results for combination of deformation methods provide convincing evidence. For example a combination of ECAE with other traditional deformation processes, such as cold rolling or hydrostatic extrusion^[114] or with hot rolling,^[70] was found to be effective. Especially effective was found a combination of ECAE with circular-to-rectangular direct extrusion.^[115] Not always, however, an extensive deformation translates to the superior thixotropic structure after partial melting.

E. Deformation-Induced Transformations in Materials

A search for optimal deformation techniques and suitable alloy compositions may lead to encounter transformations in some materials ranging beyond conventional expectations. In fact, deformation processing was found to be an effective approach to the synthesis of amorphous, nanophase and composite materials. Examples of possible outcomes are briefly signaled below.

1. Deformation-induced bulk nanostructuring

The nanocrystalline structure of a polycrystalline L12 ordered Ni₃Al alloy was induced after severe plastic deformation by HPT.^[116] It is explained that the inhomogeneous deformation leads to localized disorder and a high density of dislocations, especially geometrically necessary ones and dynamic recovery causes a heterogeneous formation of the nanocrystalline

structure. Similarly, during the cold rolling deformation of a Co-Ni-Cr-Mo alloy (MP35N) with low stacking-fault energy the nanostructures were formed, consisting of platelets of a few atomic layers in thickness and less than 100 nm in diameters.^[117] A deformation-induced nanostructuring was found in a Ti-Nb-Ta-In β alloy with low stability against α'' martensitic transformation.^[118] It is explained that the formation of fine martensite, the interaction among slip dislocations, martensite and twins, and the reversible transition from α'' back to β phase are considered as the main causes leading to pronounced grain refinement to the nanoscale.

2. Deformation-induced solid-state amorphization

The solid-state deformation offers a possibility of transforming a crystallographic structure into amorphous one.^[119] This feature is related to nanostructures described above since a broad range of nanostructured materials are obtained by processing amorphous precursor structures. An amorphization in bulk nanocrystalline nickel can be achieved by quasi-static compression at room temperature.^[120] Such structures can typically be obtained through rapid solidification. A solid-state amorphization was also achieved through HPT at room temperature in a nanostructured Al-Mg alloy,^[121] through a surface mechanical attrition treatment a nanocrystalline Al solid solution (4.2Cu, 0.3Mn) alloy,^[122] in Al₅₇Ni₁₀Ce₃ alloy deformed by repeated cold rolling and folding^[123] and in Al-Sm multilayer materials deformed through rolling and folding.^[124]

3. Deformation-induced abnormal grain growth

In contrast to above case of grain refinement, the solid-state deformation may trigger an abnormal grain growth. An example is a grain growth within the AA2195 aluminum alloy where during hot working, subgrains were formed through dynamic recovery as a result of mutual annihilation of dislocations and rearrangement of remaining ones into regular low-angle grain boundaries.^[125] Hence, the dislocation density was lower than that during cold working and was unable to restrict the abnormal grain growth.

4. Deformation-induced changes of phase composition

In addition to structural refinement, the plastic deformation may cause changes in phase composition of the alloy. During hot rolling of dual-phase steel microalloyed with Ti, a deformation affected the precipitation of titanium nitride TiN.^[126] In particular, the size of TiN precipitates generated in deformed bands was 28 pct smaller compared to those present in slabs with no deformation. The smaller TiN size contributed to grain-size reduction of austenite. Moreover, deformation led to formation of nonequilibrium phases, such as α' (HCP-structured martensite), α'' (orthorhombic-structured martensite), or ω (simple hexagonal structure phase) in certain metastable β -Type Ti-V alloys.^[127] Moreover, stress-induced α'' transformation took place in Ti-Nb-Si alloys resulting in pseudoelasticity.^[128]

Deformation is known to have a significant effect on diffusional transformations in materials. It was found that after deformation the rate of ferrite formation in steel was several orders of magnitude greater than in the absence of straining.^[129] Similarly, deformation affects the martensitic transformation in steels. Deformation-induced martensitic transformation was reported for the 304 stainless steel at different temperatures with a strain up to 30 pct.^[130] Also, deformation of Cu-Zr-(Al, Ti) bulk metallic glass composites induced a martensitic phase transformation, which resulted in strong work hardening and contributed to the large compressive deformability with plastic strains up to 15 pct.^[131]

During manufacturing of billets for thixoforming, deformation triggers recrystallization either directly or after additional heating. The melting process requires additional energy and takes place during the next step of heating to forming. There are examples, however, that stress-induced melting can occur as a transient stage during solid–solid-state transformations. For example, the solid–solid phase transformation with a large transformation strain can occur *via* internal stress-induced virtual melting along the interface at temperatures significantly (100 °C) below the melting temperature.^[132]

V. PARTIAL MELTING OF RECRYSTALLIZED STRUCTURES

During thixoforming the billet is subjected to partial melting where in contrast to conventional casting, only a fraction of an alloy volume is converted into liquid. Then, in contrast to rheo-processing, semisolid slurry is not subjected to any form of external agitation. This

excludes, for some techniques, pressures imposed on slurry to force it to flow into the die/mold cavity. In general, the microstructural evolution during partial melting is driven by the reduction of interfacial energy between solid and liquid phases and is controlled by diffusion. The plastic deformation experienced by the material prior to melting affects the kinetics of particle coarsening. There are two levels of melting investigation: (1) direct bulk measurements of transformations using thermal techniques and (2) microstructural and morphological examinations of slurry, which are done indirectly by quenching it to “freeze” the high-temperature image and then examine it at room temperature by means of a number of analytical techniques.

A. Assessing Transformations During Melting

The characteristics accompanying alloy melting including phase transitions, specific heat capacities and other important chemical properties are measured by means of differential scanning calorimetry (DSC) or simultaneous thermal analysis.^[133] In fact, the same techniques are used for measurement of changes during solidification. The thermal analysis signal in a form of heating and cooling curves is recorded during melting and solidification to calculate the temperature *vs* time and first derivative *vs* temperature. Due to its versatility and explanatory power, DSC is the most-employed thermal analysis method. The output is used to determine the alloy thermal characteristics during melting and solidification, evaluate the effect of chemical composition on metallurgical reactions, phase nucleation and growth as well as solid fraction, being the essential parameter for semisolid processing.

Thermal analysis curves provide information on liquidus, eutectic, solidus temperatures or recalescence effects (an increase in temperature that occurs while cooling metal when a change in structure). A specific physical-thermal process simulation and analytical capabilities represent instrument known as the universal metallurgical simulator and analyzer (UMSA).^[134] An example of UMSA measurements during melting/solidification of the EZ33 magnesium alloy is shown in Figure 20. The first derivatives curves shown in Figure 20(a), generally provide more detailed information related to the alloy thermal characteristics such as the liquidus, solidus temperatures or nucleation of the eutectics. The solid content *vs* temperature data obtained from measurements represent the key input for selecting thixoforming temperature (Figure 20(b)).

B. Selecting Thixoforming Temperature

When conventional casting requires overheating an alloy above liquidus, semisolid processing takes place at reduced temperatures of solidus–liquidus range, affecting a number of factors related to the process, hardware performance, alloy and product properties. A reduction of the processing temperature to the semisolid range is generally seen as the advantage of semisolid processing. Thus, selecting the processing temperature is the major task during SSP.

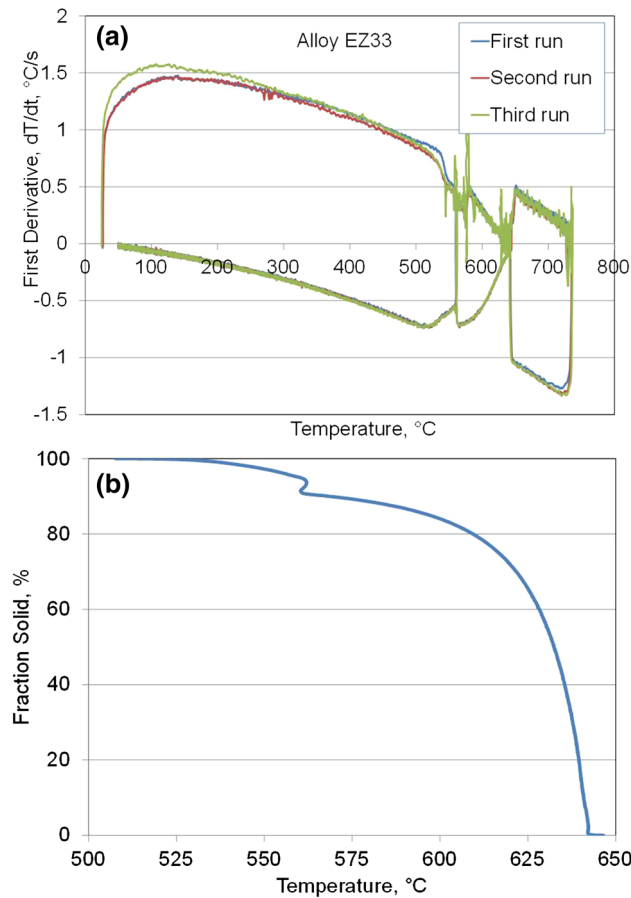


Fig. 20—Melting and solidification characteristics of EZ33 magnesium alloy determined using the universal metallurgical simulator and analyzer (UMSA): (a) first derivatives of heating and cooling curves vs temperature for three experimental runs; (b) plot of solid content vs temperature.

1. Alloy degradation and hardware performance

An inherent feature of some alloys (e.g., magnesium) is their very high affinity to oxygen. Thus, at high temperatures, especially that corresponding to semisolid or liquid states, molten alloys exposed to an oxidizing atmosphere react rapidly leading to oxidation or in some cases to ignition and combustion.^[75,76] Although casting and forming in the solidus–liquidus range create an impression of reduced energy consumption, to reach the final conclusion, all elements of the manufacturing cycle should be considered. The process economy is affected by the hardware required and its service life. The processing temperature affects not only thermal attack but also chemical reactivity of the molten alloy. It is generally concluded that a reduction in processing temperature is universally positive and sometimes lowering temperature by 20 °C to 30 °C makes a substantial difference in service life of the hardware.^[135]

2. Solid fraction effect on product integrity and properties

The solid fraction is the key parameter affecting the viscosity of the semisolid slurry. It can be directly measured on rapidly quenched samples, using metallographic techniques, such as line intercept^[136] or by

thermal analysis exploring melting solidification curves.^[137] Alternatively, for simple alloy systems the solid fraction is determined based on phase diagram.

For a binary alloy that melts and solidifies under equilibrium conditions the weight of solid fraction f_S^{Eq} at a processing temperature T is calculated^[138,139]:

$$f_S^{\text{Eq}} = \frac{(T_M - T) - m_L c_o}{(T_M - T)(1 - k)}, \quad [3]$$

where T_M is melting temperature of the pure solvent, m_L is the slope of the liquidus line, c_o is composition of the alloy and k is partition coefficient of the alloy.

For nonequilibrium solidification with diffusion occurring only in the liquid phase with no diffusion in the solid phase the weight of solid fraction f_S^{Sch} is expressed by Scheil's equation^[138,139]:

$$f_S^{\text{Sch}} = 1 - \left(\frac{T_M - T}{T_M - T_L} \right)^{\frac{1}{1-k}}, \quad [4]$$

where T_L is the liquidus temperature of the alloy.

3. Internal integrity

The evident concern during conventional casting is an internal integrity of the product. The high part integrity achieved through semisolid methods improves properties in the as-cast state and also allows their modification by exploring heat treatment.^[140] There is a general expectation that higher solid fraction will lead to less defects associated with solidification. In this respect, the lower temperature within the semisolid range will cause reduced porosity due to lower shrinkage and better part filling due to the laminar flow. While this is true for solidification shrinkage, the frequency of other defects may increase due the fact that the reduced heat content of the slurry shortens the metal flow length and makes it prone to premature freezing, before reaching its position inside the die. To compensate this, hot runners are required instead of conventional cold runners, which represents at present a technological barrier.^[1] So far, such solutions are only available for transport of molten plastics.

4. Component properties

A reduction of the processing temperature during thixoforming influences a number of factors that affect solidification characteristics and the final microstructure. While some factors cause an improvement in product properties, others have clearly negative contribution. According to the general rule, refining microstructural components leads to improved properties and is highly desirable. For the liquid alloy portion, a refinement is achieved by an increased cooling rate. The cooling rate, however, does not affect the size of the primary solid particles.

The role of the processing temperature within the solidus–liquidus range in material properties is more complex and there is no consistent evidence supporting the general expectation that its reduction leads to improved properties. For presently processed magnesium alloys, there are examples showing exactly the

opposite behavior where increased solid fraction led to reduced both the strength and ductility.^[141] As a further evidence, there is a finding for Mg-Al and Mg-Al-Zn alloys that the highest strength and ductility were obtained for near-liquidus processing with 0 pct of solid fraction.^[142, 143] To reverse this trend, recent efforts within both the industry and academia focus on identifying opportunities at different stages of the manufacturing cycle (*e.g.*, post-forming treatments) that could create the beneficial microstructure. Since thixotropic mixtures represent a form of reversed composites with the primary solid being a softer phase than the matrix, minimizing the globule size is of crucial importance.

C. Morphological Characteristics of Thixotropic Slurry

When transforming dendritic structures into new morphologies, commonly described as nondendritic ones, the question arises what is the optimal shape of the primary solid required for successful processing. As opposed to rheo-processing route when nucleation from the liquid phase is the mechanism influencing the growing solid, during thixo-processing route reviewed in this report, the solid remains as an alloy (billet) portion which does not completely melt during preheating to thixoforming. The unmelted solid influence depends on its content within the melt, which in some cases may exceed 80 pct, emphasizing importance.^[41] While considering the role of solid fraction, two aspects should be distinguished. First, at temperatures of semisolid range the solid controls rheological properties of the slurry. Then, after solidification it affects properties of the final product. Below, major characteristics of the solid particles are described.

1. Size of the solid particles

The particular attention during partial melting is attributed to the size of primary solid particles. During rheocasting, the size of the primary solid is controlled by the nucleation rate and increasing a number of nucleation sites available allows its refinement. During thixoforming, the size of the solid globules originates from the grain size in the solid state after recrystallization.^[144] As shown in Figure 21, the final particle size is many times larger than the initial grain, reaching typically over 100 μm .^[36] Such a large size is detrimental to material properties.

In the absence of external strain, the reduction of interfacial energy between the particles and liquid provides the key driving force for morphological and dimensional changes with a contribution from coalescence and Ostwald ripening.^[145,146] The coalescence describes the nearly instantaneous formation of one large particle upon contact of two smaller ones. Ostwald ripening is governed by the Gibbs–Thompson effect, which alters the concentration at the particle–matrix interface, depending on the curvature of the interface. The particle curvature creates the concentration gradient for the diffusional transport of the material.^[147] Ostwald ripening is a paradigm for statistical self-similarity in coarsening systems and the first quantitative

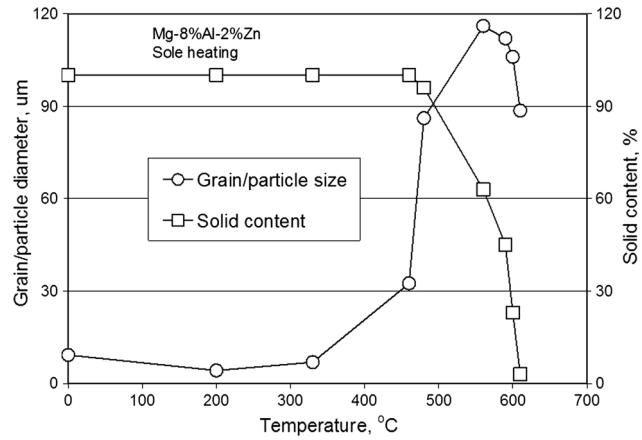


Fig. 21—Diameters of grains (in solid state) and solid particles (in semisolid slurry) as a function of temperature for magnesium alloy extruded at 200 °C plotted along solid content. Reprinted with permission from Ref. [35].

description of this phenomenon was given by Lifshitz and Slyozov^[148] and Wagner.^[149] Today it is known as the classical LSW theory.^[148, 150] Many factors were identified in the literature to affect the size of solid particles in the slurry.

a. Effect of solid-state deformation on particle size

According to experiments with the AA2014 aluminum alloy the coarsening rate was affected by technique of slurry preparation.^[151,152] A slightly lower coarsening rate was observed for RAP route of the AA2014 alloy with 37 pct liquid fraction than for the *cooling slope method* treatment of the same alloy with 17 pct fraction liquid, despite the higher liquid fraction. For the cooling slope technique, an increase in liquid fraction gave a higher coarsening rate. It is likely that relatively low coarsening rates are associated with the presence of fine solid compounds, which are inhibiting the migration of liquid film grain boundaries, either through a pinning mechanism or through impeding diffusion through the liquid film at the boundary.

An increasing compression ratio during cross wedge rolling from 10 to 30 pct reduced the solid particle size of the A356.2 alloy at 580 °C from over 90 μm to around 70 μm . A role of deformation ratio is also reported for the AZ91D alloy, where after 4 pass ECAE at 225 °C with an equivalent strain of 3.63, holding at 545 °C for 25 minutes resulted in the solid particle size of 5 μm .^[153] For upsetting at 225 °C with deformation of 30 pct (strain equivalent 0.3), the same AZ91D hold for 25 minutes at 545 °C developed the solid particle size of 180 μm . It should be mentioned that the size of solid particles of 5 μm as reported in Reference 153, is the smallest one found in the literature. However, the optical microscopy evidence for small particles with a diameter in the range of 2 to 5 μm is not fully convincing. The LSW theory was used to describe the coarsening process of semisolid slurry after compression deformation through RUE in a Gleeble-1500 thermal–mechanical simulator of the AA7075 aluminum alloy at 250 °C.^[28] After examination of the billet

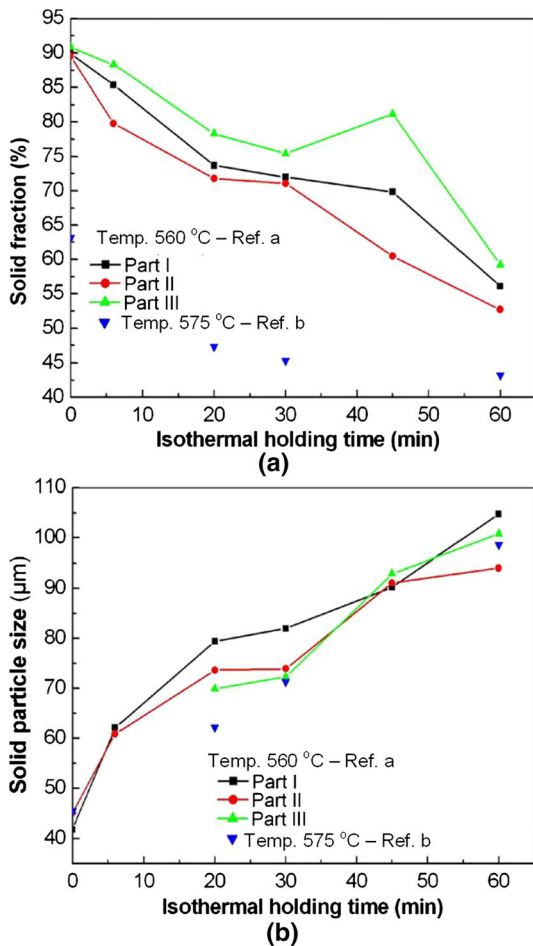


Fig. 22—The solid fraction (a) and solid particle size (b), plotted as a function of the isothermal holding time. The line and symbol denote the data in this study. Ref. [24] (a); Ref. [257] (b). Reprinted with permission from Ref. [24].

reheated to a range of 580 °C to 620 °C and holding for 2 to 35 minutes, it was concluded that the increasing number of RUE cycles accelerated the recrystallization rate, reduced the average particle size, and improved the degree of their spheroidization.

b. Effect of holding time in semisolid range on particle size

For the AZ91D magnesium alloy asymmetrically deformed by compression at 230 °C, isothermal holding in semisolid range affected both the content and size of solid particles.^[24] During isothermal holding, recrystallization was followed by liquid phase nucleation occurring first in the heavily deformed regions. With the passage of time, solid fraction decreased, while solid particle size increased in all regions despite of deformation (Figure 22). After holding for 20 minutes, the anisotropy caused by asymmetric deformation was reduced. The influence of holding time in solidus–liquidus range was also documented for extruded AZ80 magnesium alloy. As shown in Figure 23, after 5 minutes holding, the homogeneous semisolid slurry was formed and further holding only led to undesirable grain growth.^[154] The size of the solid particles reached about

60, 80, and 160 µm for holding times of 0, 5, and 60 minutes, respectively. Also for the A356.2 alloy deformed by cross wedge rolling, holding at 580 °C for 5 to 20 minutes first reduced the solid particle size but after 10 minutes caused its coarsening.^[155]

The experiments with the A319 aluminum alloy led to conclusion that the effective method to obtain desirable microstructure is to manage the time in the semisolid state by controlling heating rate and soaking time.^[156] The coarsening rate of 227 µm³/s was obtained during isothermal testing.

c. Effect of grain refiner or other additives on particle size

The size of solid particles depends on grain refiner added to the alloy and the extent of deformation. For 0.02 pct additions of the Ti (Al-5Ti-1B) refiner to the AA6070 Al alloy, the increasing pre-deformation reduced the globules size and increased their sphericity with the optimal temperature, holding time, and strain fixed at 630 °C, 20 minutes and 30 pct, respectively.^[157] For these processing parameters, the average globule size achieved minimum values of 68 and 55 µm for the unrefined and 0.02 pct Ti-refined alloy, respectively. The effect of Al5Ti1B grain refiners was also studied for the AlZnMgCu alloy subjected to SIMA at 300 °C with deformation ratio of 40 pct.^[158] The optimal level of Ti was found to be 0.1 pct. Significant improvements in mechanical properties were obtained with additions of grain refiners combined with T6 heat treatment.

For the extruded AZ80 magnesium alloy, small additions of Y (up to 0.8 pct) were found to control particle coarsening.^[159] The coarsening rate constant of AZ80 with 0.2 pct Y addition, of 164.22 µm³/s was approximately four times less than the un-modified AZ80 alloy of 689.44 µm³/s. Although extending isothermal holding in semisolid range improved generally the particle sphericity, there is an evidence of opposite changes. For example, during deformation of the AZ31B alloy by compression of 28 to 30 pct at 300 °C, long holding at temperature of 600 °C to 630 °C led to irregular shape of solid particles.^[160]

2. Shape of the solid particles

During thixoforming the particle shape will arise during melting of the billet and then due to interaction with neighboring particles during holding and during flow into the die cavity. These conditions are different than that during rheo-processing. Therefore the morphological transition from dendrites to rosettes and spherical shapes with increasing shear and intensity of turbulence as it is the case during rheo-casting will not apply here.^[39]

When properties of the slurry in solidus–liquidus range and then solid alloy after solidification are governed by three-dimensional particles, their assessment is done on flat metallographic sections for two-dimensional features. So the question arises on correlation between 3D and 2D images. An example for Al alloy in Figure 24 shows differences between the complex 3D shape and their simplest 2D planar sections.^[161] The particles appearing near spheroidal on planar sections

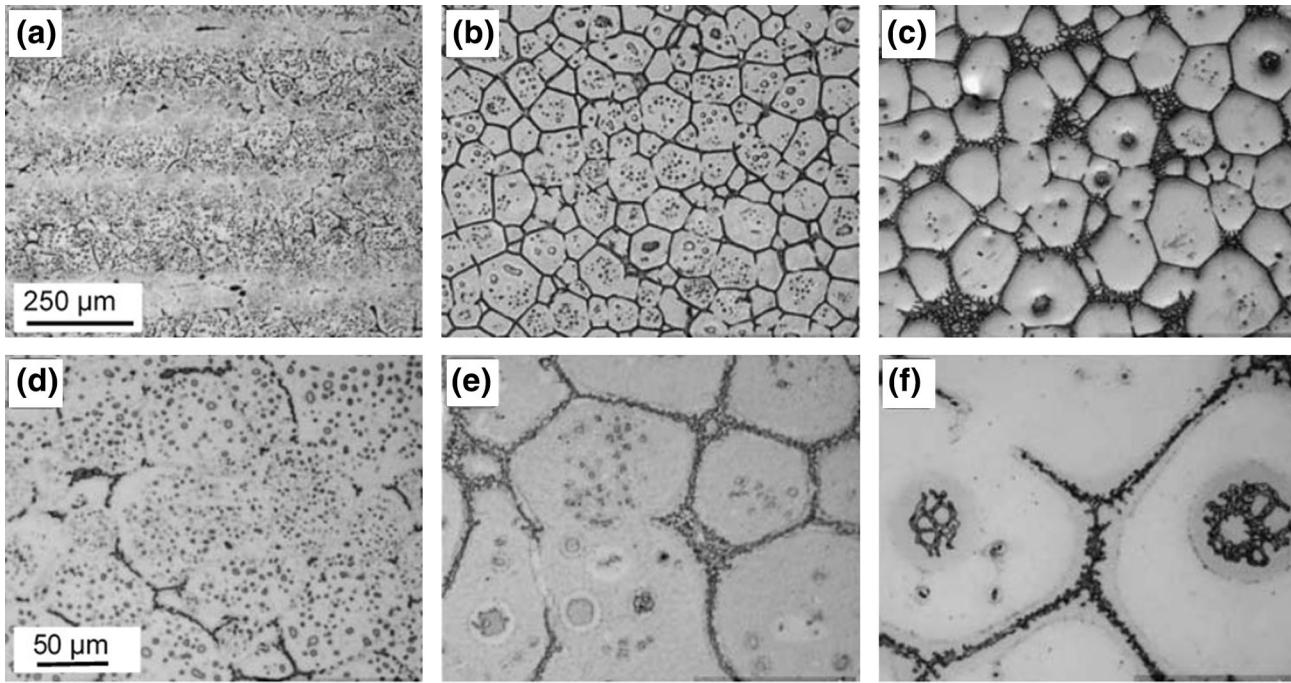


Fig. 23—Microstructure of AZ80 reheated to 570 °C and isothermally held for (a, d) 0 min, (b, e) 5 min and (c, f) 60 min. Reprinted with permission from Ref. [154].

are in fact of complex 3D shape. Some of them are interconnected with surrounding particles, forming complex-shape conglomerates. The average sphericity (roundness) of particles is expressed by shape factor F_s :

$$F_s = \frac{1}{n} \sum_{n=1}^n \frac{L^2}{4\pi A}, \quad [5]$$

where n is the number of solid particles, L is the perimeter length, and A is the area as seen on the cross section. Hence, when F_s equals 1, the particle is perfectly round. A different roundness indicator, calculated as $1/F_s$, is also used.

An experimental research and modeling suggest that the solid shape in the slurry is affected by solid-state deformation prior to melting and, in general, the sphericity is reported higher than that after liquid-state agitation. For example, during deformation of the AA7075 aluminum alloy, the optimal shape was obtained for the effective strain of 5.1, holding temperature of 609 °C and time of 14 minutes.^[162] For the A356.2 aluminum alloy deformed by cross wedge rolling, increasing compression ratio from 10 to 35 pct increased the shape factor of solid particles at 580 °C from 0.5 to over 0.65.^[155] Similarly, holding time at temperature of semisolid range of 580 °C increased the shape factor of solid particles.

There is a research comparing the influence of liquid agitation techniques as electromagnetic stirring, solidification time, modification of the eutectic and grain refinement and solid-state thermomechanical treatments prior to partial remelting (like solutionizing and cold rolling) on the solid particle shape.^[163] Hence, for the

Al-Si7Mg alloy cold working prior to partial remelting resulted in the most rapid generation of the perfectly globular morphology of solid particles, once the threshold deformation for recrystallization was exceeded. Moreover, the size of solid particles was not affected by the initial microstructure. The particle coarsening rate during isothermal holding was lower than that obtained after the electromagnetic stirring of the same alloy.

3. Chemical and phase composition of solid particles

A simplified description of semisolid slurries frequently distinguishes just solid and liquid phases. However, the solid particles may represent multiphase systems with complex structure. Their phase composition may be deduced from phase diagrams for equilibrium or nonequilibrium (Scheil) cooling conditions, e.g., calculated using the FACTSage software.^[164] At semi-solid range, solid particles itself may represent a mixture of solid and individual liquid pools distributed within. A specific feature of solid particles at temperature of semisolid range is the so-called entrapped liquid (Figure 25). As seen in a case of liquid pool in Figure 25a and grain boundaries in Figure 25b, using term “grain” for solid particles may not be accurate.

Many investigators have studied the microstructural evolution during partial melting and found a presence of small liquid pools within primary particles.^[165] At solidus–liquidus range, the liquid pools within solids reduce the volume of liquid surrounding solid particles, negatively affecting the slurry flow. The formation mechanism and evolution of liquid pools entrapped within solid particles were investigated during partial

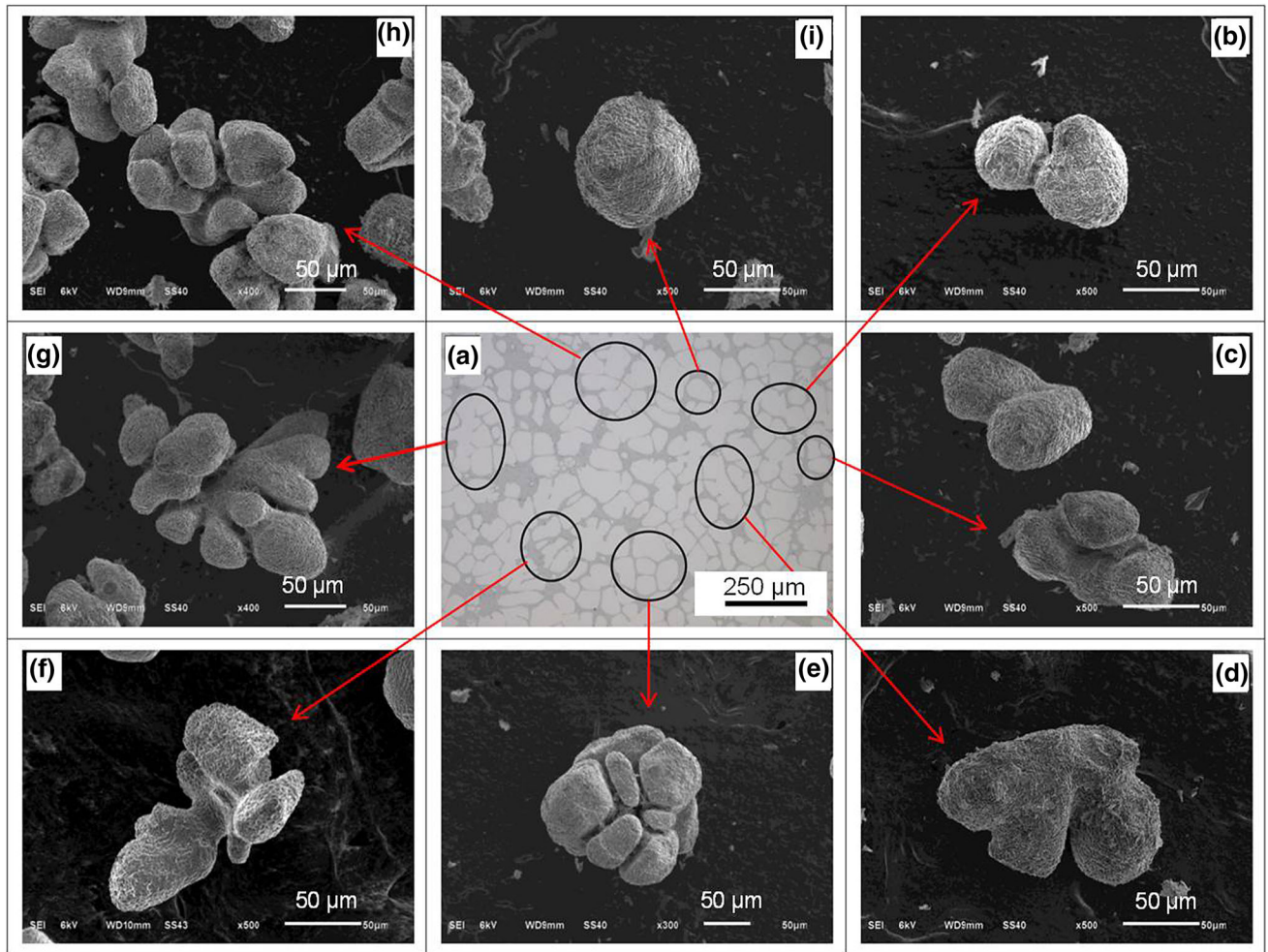


Fig. 24—General microstructure of the rheo high-pressure die cast A356 alloy in the as-cast condition shown on planar 2D section (a) and accompanying 3D images of extracted grains from the casting locations indicated by arrows (b through i). Reprinted with permission from Ref. [161].

melting of the $Mg_2Si/AM60B$ composite with fine-grains.^[166] The results indicate that merging of dendrite arms during the initial stage of partial melting is the main cause for the formation of the entrapped liquid pools. According to phase transformations the generation of the entrapped liquid pools is attributed to the reactions of $\alpha + \beta \rightarrow L$ and $\alpha \rightarrow L$. As shown through *in situ* X-ray micro-tomography examinations during partial melting of the cold-rolled Al-8Cu alloy, the liquid droplets entrapped inside solid globules nucleate and coarsen.^[167]

VI. SOLIDIFICATION OF SEMISOLID SLURRIES

After thixoforming is completed, the remnant liquid is subjected to solidification. Its volume fraction and chemical composition depend on processing parameters. Thus, during partial melting, the primary focus is on the morphology of solid fraction, while during solidification, the liquid fraction attracts the major attention.

A. Chemical Composition of the Remnant Liquid

In semisolid slurry, the chemical composition of the remnant liquid is different from that of the average composition of the alloy and the lower liquid fraction is accompanied by the larger differences. For a given alloy chemistry, the composition of the liquid fraction depends on temperature within the solidus–liquidus range. As shown in Figure 26, for a simple phase diagram, the lower temperature is accompanied by higher content of the lower-melting-point element. Thus, the regions between dendrites are rich in the lower melting-point element, since these regions represent the last liquid to solidify. A lack of physical agitation during thixoforming affects the solidification mechanism of remnant liquid. In particular, during thixocasting of the AA7075 aluminum alloy, the liquid pools transformed back into dendritic morphologies.^[168] Then, the dendritic solidification is accompanied by recrystallization, solute distribution, ripening, interdendritic fluid flow, and movement of solid.^[169]

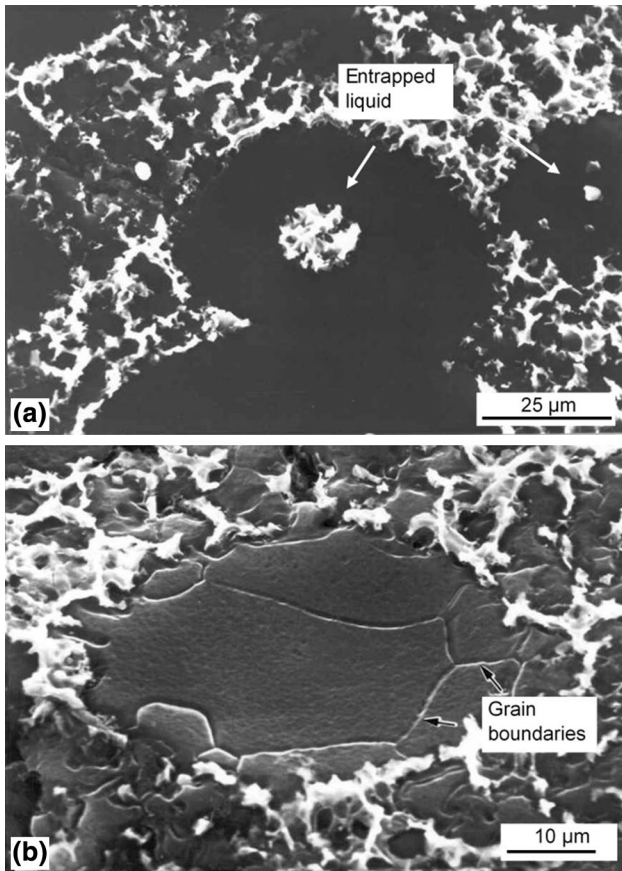


Fig. 25—SEM images of primary solid particles in AZ91D alloy processed from coarse particulates deformed by mechanical comminuting: (a) particle containing in the centre a solidification product of “entrapped liquid”—alloy containing 43 pct of the primary solid; (b) particle without any precipitate of a second phase with grain boundaries in near-surface region—alloy with 5 pct of the primary solid. Surface after Ar ion etching. Reprinted with permission from Ref. [141].

B. Solidification Features

After solidification, the liquid fraction that transforms into a solid, connects the primary solid in the final product. Its properties are, therefore, essential for entire microstructure, created during semisolid processing. As documented by fractographic observations, the interface between the primary solid and solidified liquid fraction represents a weak region leading to crack-propagation path during alloy failure.^[141] Thus, there are efforts oriented toward controlling properties of the solid-liquid interface. In addition to chemical composition that may cause embrittlement, the remnant liquid solidification areas are prone to solidification defects, as is the case in cast structure. As a major concern, there is a solidification shrinkage since there may not be sufficient amount of molten alloy to feed the remaining volume behind the moving solidification front.

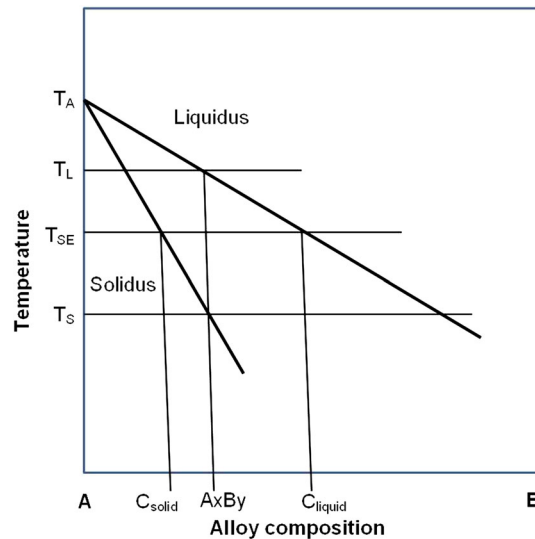


Fig. 26—Schematics showing a composition of remnant liquid during solidification of semisolid slurry.

VII. ALLOYS FOR THERMOMECHANICAL ROUTE OF BILLET PREPARATION

Alloys to be applicable for semisolid processing have to fulfill general criteria.^[170] An additional condition required for thixoforming with a billet prepared by the solid-state deformation route is the alloy formability. Over decades a variety of alloys were explored both at laboratory and industrial scales mainly based on Al, Mg, Zn, Cu, Fe (steel) or Co. Experiments with metal matrix composites were also carried out. A recent trial included new materials called high-entropy alloys (Table II).

A. Cast vs Wrought Grades

The predominant portion of presently used alloys for thermomechanical route of billet preparation belongs to casting grades. Among them, the most often used are aluminum casting alloys A356 or A357 with good fluidity and castability due to high content of Al-Si eutectics. For copper grades the ZCuSn10 alloy was used for the billet preparation through rolling and partial melting.^[95]

There is an interest in alloys designed for wrought processing, known of having better performance and offering higher mechanical properties than cast grades.^[171] This is in part due to lack of alloys specifically designed for semisolid processing. According to experimental trials, the high-strength wrought aluminum alloys can be thixoformed. However, wrought alloys are more difficult to process due to low content of eutectics and narrow solidification range, sometimes limited to a few °C. Moreover, the usually wrought high-strength aluminum alloys, which are typically used in forging, are not well suited for semisolid forming, especially because they have a tendency for hot cracking

during solidification. Therefore, the superior mechanical properties of forged components cannot completely be achieved by thixoforming. It appears that some modifications to composition or some tighter constraints in the bounds allowed in the alloy specification are required. The most frequently thixoformed alloys designed for wrought processing include AA6061, AA6066, AA2024, AA7075 aluminum, C544, C360 copper, or steel.^[17,18]

B. Utilizing Alloys in As-wrought State

There is an ambiguity in the literature regarding use of wrought alloys for thixoforming. It is caused by the fact that these alloys are not only used for billet manufacturing in initial as-cast state^[16] but also in initial wrought state.^[172] In some papers, the initial state is left not specified or described as “as-supplied,” leaving the reader guessing. Using a wrought-state precursor without specifying the initial structure may lead to misleading conclusions that just melting (with omitting deformation treatments) is generally sufficient for converting dendritic forms into thixotropic structures. Therefore, for clarity, the *as-wrought state* term is used in this paper to distinguish it from alloys designed for wrought processing but being in the *as-cast state*. Since the objective of thermomechanical treatment during billet preparation is to convert dendritic forms present after casting into nondendritic morphologies, according to this definition, the SIMA, RAP and Woodhouse concepts do not apply to materials being already in the wrought state. Being in a wrought state means that an alloy was already subjected to thermomechanical treatment.

Using the as-wrought alloys and then subjecting them to partial remelting either directly or after additional thermomechanical processing does increase the number of manufacturing steps and component cost. Although it may be easy and convenient for laboratory experimentations, in reality, remelting of quality wrought structure is expensive since cost of the entire manufacturing cycle should be calculated. Therefore, partial melting of the as-wrought alloys may find justification for a limited volume niche market but does not have characteristics required for a technology suitable for mass-scale production.

1. Direct partial melting of alloys in the as-wrought state

Direct partial melting is promoted as being effective for high-melting-point alloys, mainly steels. Since the wrought state involved intensive, often multistage, deformation during manufacturing, alloys have deformed (or also recrystallized) microstructure ready for partial melting.^[172–176] Direct partial melting experiments involved tool steels such as M2, D2, and XW-42.^[174] In case of D2 steel, the process started from the soft annealing state at 850 °C.^[176] The material was heated in an argon atmosphere up to 1330 °C which corresponded to about 38 pct of liquid fraction and held for 5 minutes followed by air cooling to room temperature. As shown in Figure 27, after partial melting, the microstructure consisted of globular particles with an

average size of about 50 μm , while the areas between globules were filled with eutectic carbides forming a lamellar network.

2. Applying solid-state deformation to alloys in the as-wrought state

There are examples when alloys in the as-wrought state are additionally subjected to hot, cold deformation or their combinations, preceding partial melting.^[177,178] In principle, extra deformation steps may be added to the already as-wrought state of the material to increase deformation. However, an additional deformation treatment of wrought alloys multiplies the already high-manufacturing cost and is not viable economically.

An example is shown for the AA2024 alloy where open die forging (upsetting) with strains from 0.1 to 1.0 was used to deform cold-rolled bars. The increased cold strain caused reduction of the grain size from 76 to 52 μm .^[179] In another research, the commercially wrought 2024 aluminum alloy T4 rods were annealed at 415 °C for 3 hours, cold compressed at 40 pct reduction and partially melted at 620 °C (55 pct liquid fraction) leading to α grains with diameter of 88.2 μm surrounded by eutectics.^[180] For the AA7075 Al alloy the RUE at 250 °C was used to produce billets. After reheating to 580 °C to 620 °C for 2 to 35 minutes, the fine and spheroidal morphology was developed.^[28] Before melting, the grain-boundary composition approached Al-Cu and Al-Si binary eutectics with the increased contents of Cu and Si and reduced content of Mg. It was found that the three-cycle deformation by RUE followed by isothermal heating at a temperature range of 600 °C to 610 °C for 10 to 15 minutes provided an optimal microstructure in terms of size and shape of spheroidal features. Further deformation caused microstructure degradation through increased size and reduced sphericity of solid particles. These findings suggest that the optimal rather than the maximum deformation is required. However, there is an invention proposing hot extrusion at 540 °C (42 °C below solidus) for the cold-rolled AA6061 aluminum alloy as the treatment optimizing properties of the billet.^[27]

For wrought alloys it is important to test partial remelting before application of additional deformation to assess viability of increasing the manufacturing cost. An influence of additional deformation was assessed for the AA6063 aluminum alloy in the form of an as-extruded bar.^[178] As shown in Figure 28(a), the initial microstructure is typical for extruded state with fibrous grains and intermetallic particles aligned in the extrusion direction. After direct partial melting at 630 °C, the billet developed large and irregular solid grains with possible adverse effect on the mechanical properties (Figure 28(b)). A deformation by a combination of radial forging at 300 °C with 70 pct area reduction followed by unidirectional forging at room temperature and compression ratio of 80 pct showed refined grains with no evidence of recrystallization (Figure 28(c)). Partial melting of additionally deformed structure at 630 °C led to solid particles with a size of over 100 μm (Figure 28(d)). While this example shows beneficial

Table II. Examples of Alloys Used for Thixoforming, Utilizing Billets Manufactured by Solid-State Deformation Prior to Melting to Generate Globular Morphologies

Alloys	Base	Major Chemical Elements (Wt Pct)	Cast/Wrought	Specific Gravity (g/cm ³)	Liquidus (°C)	Solidus (°C)	Thixoforming Refs.
A356.0	Al	7Si-0.3Mg	cast	2.7	615	555	192
6061	Al	0.8 to 1.2Mg, 0.4 to 0.8Si	wrought	2.7	652	582	18
7075	Al	2.1 to 2.9Mg, max 0.4Si, 0.18 to 0.28Cr	wrought	2.8	635	477	11, 20
ZA27	Zn	27Al, 2Cu	cast	5.0	484	376	165
AZ91	Mg	9Al, 1Zn	cast	1.8	595	470	15, 153
AM60	Mg	6Al	cast	1.8	615	540	197, 206
ZK60	Mg	6Zn, 0.5Zr	wrought	1.9	635	520	210
C360 Brass	Cu	3Pb, 35.5Zn	wrought	8.5	899	888	11
AISI H13 Steel	Fe	0.36C, 5.26Cr, 0.8V, 1.2Mo	wrought	7.7	1454	1315	200
M2	Fe	0.78C, 3.7Cr, 1.7V, 4.5Mo, 5.5W	wrought	8.1	1425	1235	32
Stellite 21	Co	62Co, 27Cr, 0.25C, 5.5Mo, 2.7Ni	cast	8.3	1366	1338	71
Composite	Al	Al 6061 matrix + SiC reinforcement particles	cast		652	582	247
High-entropy Alloy		CoCrCuFeNi (equiatomic contents)	cast				248
High-entropy Alloy		AlCoCrCuNi (equiatomic contents)	cast		1325	1085	196

effect of additional deformation, there is vast evidence proving similar effect achieved after just a single-step deformation.

C. Low Formability Metals

The material formability is an essential feature qualifying it for thermomechanical way of billet preparation. It is obvious that alloys with poor formability may crack providing a limited success. Some improvement of formability may be achieved by increasing the deformation temperature, applying annealing between passes and reducing deformation within a single pass.^[181] Thus, metals with BCC and HCP structure would benefit from methods relying on temperature exceeding recrystallization. In contrast, metals with FCC structure, known to have good formability, may rely on deformation below the recrystallization temperature. In addition to the alloy matrix, its formability may be degraded due to the presence of continuous and brittle intermetallic compounds along with the formation of eutectic structures at grain boundaries. To some extent, the formability improvement may be achieved through changing deformation conditions as is the case in superplastic forming, ECAE, cross-roll rolling, asymmetric, or shear rolling.

Examples of alloys frequently used in semisolid processing but having poor formability are magnesium-based grades. The poor plastic flow properties of magnesium at room temperature are inherently related to its crystal anisotropy and HCP structure offering limited number of active slip systems, primarily just involving the basal planes.^[1] The critical resolved shear stress for basal plane slip in magnesium single crystal is about two orders of magnitude lower than that for nonbasal plane slip involving prismatic or pyramidal planes so the distribution of the former plays an

important role in determining its formability. Therefore, deformation resistance along direction parallel to the basal plane is small, but deformation resistance in direction parallel to the prismatic plane is very large. As explained in Figure 29, due to strong preferred crystallographic texture, during rolling, a metal cannot deform along the thickness direction. Since during rolling deformation, very strong basal texture develops in magnesium sheet, changing the texture type, or at least weakening of the basal component, is an effective route to formability enhancement.

D. Improving Formability Through Alloying

In the case of magnesium alloys, the effective way of improving formability is through modification of their chemical composition. Recent studies^[182] have shown that magnesium when alloyed with rare earth elements developed much weaker basal texture resulting in improved room-temperature formability. In addition to weakening the basal texture and improving ductility, the advantages of rare earths include high strength, high creep resistance, acceptable corrosion behavior, and improved flammability resistance. As an explanation, it is proposed that a strong interaction of solutes with dislocations and grain boundaries is responsible for the significant impact rare earth additions have on the extruded grain size and texture at very low alloying levels. Since rare earths are associated with the high-cost and supply issues, there are trials with other elements having high affinity to oxygen as Ca, Sr, and Ba.^[183,184] An interesting finding is a synergy of certain elements, *e.g.*, a combination of Ca and Ce, which enhanced precipitation hardening, refined grain size, improved texture, and ductility to greater extent than is the case with the separate additions of individual elements.

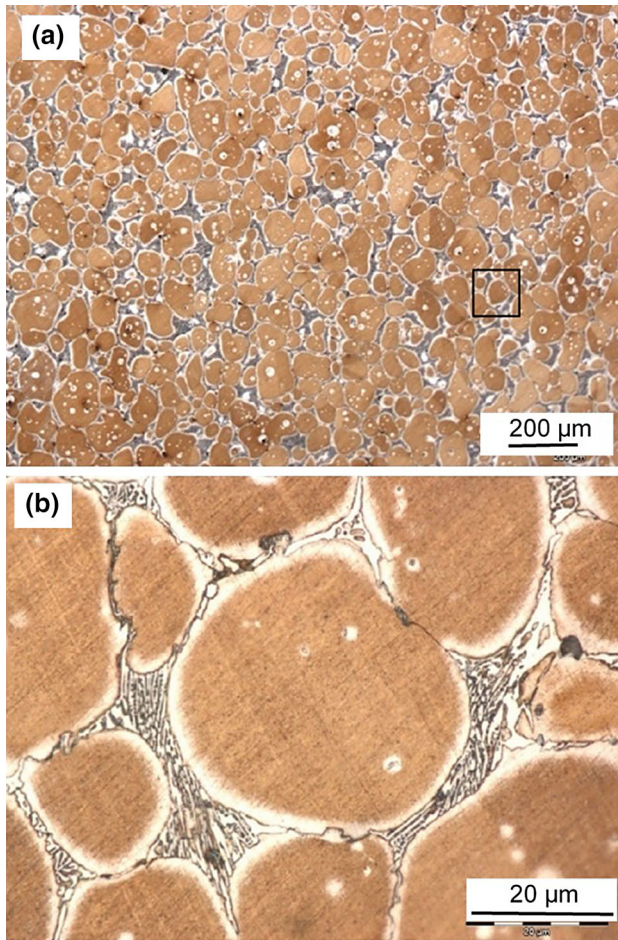


Fig. 27—Microstructure of AISI D2 steel after direct partial remelting from the as-wrought state at 1300 °C, holding for 5 min and air cooling: (a) general view; (b) magnified image showing structure of solid/solid interface. Reprinted from Ref. [173].

VIII. DEFORMATION-ENHANCED MELTING OF COARSE PARTICULATES

In addition to bulk billets used in thixocasting or thixoforging, there is also feedstock in a form of coarse particulates used as a material precursor for net-shape semisolid forming. These are relatively coarse particulates with a size of several millimeters, which are orders of magnitudes larger than particles of tens or hundreds of micrometers used in powder metallurgy.^[185] Although there is a size difference of orders of magnitude between the bulk billet and coarse particulates, the thermomechanical treatment prior to melting plays the same role in dendrites–globules transformation within both types of the feedstock.

A. Coarse Particulates

Coarse particulates are either deliberately manufactured by mechanical comminuting of cast ingots or collected as byproduct during machining of components. To manufacture chips, the material passes through rolls with cutting teeth located around their surfaces. After cutting, chips are separated based on size

using sieving.^[1] An example of chip morphology, manufactured from zinc and magnesium alloys, is shown in Figure 30.

An alternative route of billet manufacturing explores solid-state compaction of coarse particulates (chips). In the case of chips generated during part machining, this route offers an effective way of metal recycling. According to Reference 85, chips of the AZ91D magnesium alloy were subjected to series of isothermal treatments for various holding times within the range of 510 °C to 570 °C following compression into a billet at 250 °C. The outcome was a semisolid structure with the highly spheroidal and homogeneous solid particles. A similar idea of recycling of the AZ91D magnesium alloy chips to produce the semisolid billet is described in Reference 86. Moreover, the machined chips were used as a precursor in billet preparation from AZ91 and AZ31 alloys.^[87] The manufactured billets developed refined and globular primary α -Mg solid particles with sizes of about 55 μm for the AZ91 and 50 μm for the AZ31 alloy. In another recycling idea, the AA6060 aluminum alloy chips were compacted into billets and then extruded through the flat-face, porthole, and ECAP dies to impose different deformations.^[186] The high-quality aluminum billets, manufactured this way, may be used for semisolid processing. The compaction of billets using deliberately comminuted chips does not seem to be economically viable. There are, however, examples of laboratory scale experiments where chips deliberately produced from the ADC12 aluminum alloy (10.7Si, 2.3Cu) by lath machining were compressed inside a mold at 200 °C.^[187] After partial melting at 555 °C, the billet developed homogeneous and spherical particles with the average size of 82 μm .

The chip recycling technology combined with the SIMA method, called CR-SIMA, was adopted to prepare semisolid billets from the AZ91D magnesium alloy refined by Er additions.^[88] After chip compaction, the microstructure consisted of fine α -Mg grains and the γ -Mg₁₇Al₁₂ phase quite uniformly dispersed within the matrix. During continuous heating, the γ -Mg₁₇Al₁₂ phase distributed at triple junctions melted, and grains were separated. During the semisolid isothermal holding, the amount of liquid increased until the solid–liquid system reached its equilibrium state. At the same time, the particles gradually spheroidized and began to grow with the further increasing holding time. As a result, semisolid microstructure with small and spheroidal primary particles was obtained.

B. Melting Characteristics of Coarse Particulates

The chips manufacturing using mechanical cutting, which takes place at temperature below 100 °C resulted in cold work within their entire volume.^[1] Although it is difficult to estimate quantitatively the extent of chip deformation, in general the internal structure exhibits all features typical of heavily deformed material. As explained in detail in Reference 36, the heating of the mechanically chipped alloy led to essential changes within its microstructure, expressed primarily by a replacement of cold-deformed structure by strain-free

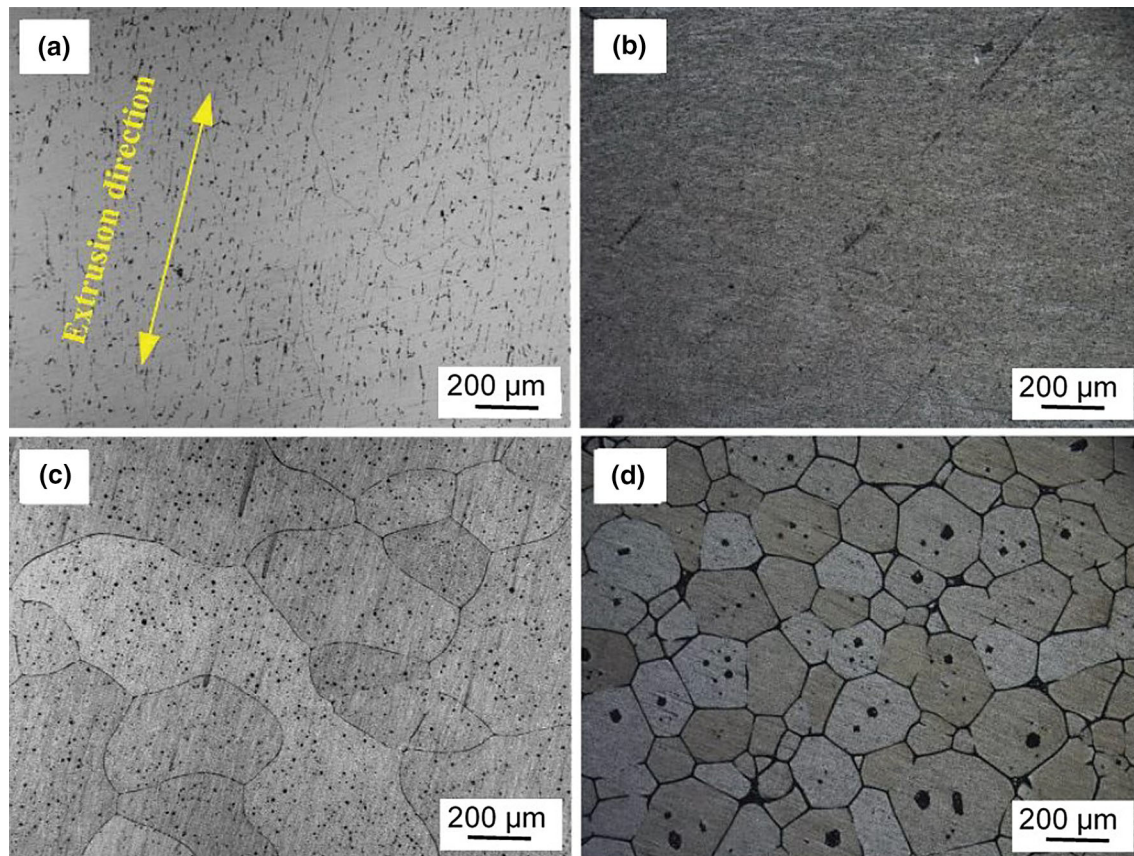


Fig. 28—Effect of additional deformation on microstructure of AA6063 aluminum alloy after partial melting: (a) the as-extruded state; (b) the as-extruded and partially melted at 630 °C and 15 min holding; (c) the as-extruded and radially forged at 300 °C with 70 pct area reduction and compressed at room temperature with 80 pct of compression ratio; (d) after partial melting of (c) at 630 °C and holding for 15 min. Reprinted from Ref. [178].

grains. Exceeding the solidus temperature activated an alloy melting and transformed an equiaxed grain structure into semisolid slurry. An example of heating of deformed magnesium alloy particulates is shown in Figure 31. In the same figure, an analogy is shown in terms of behavior of globules from the same alloy, created during rapid solidification. During the very initial stages of the alloy melting, the network of grain boundaries was covered with the liquid phase, which at room temperature represents a practically pure $Mg_{17}Al_{12}$ compound. As the temperature increases, the equiaxed grains transformed to spherical solid particles, surrounded by the liquid phase. Thus, a combination of cold deformation, introduced during chipping, and recrystallization during subsequent heating control the thermal decomposition of chips during melting.

An example of direct application of coarse particulates is a commercial semisolid technology of injection molding (thixomolding) where particulates are fed into a machine similar to that used in molding plastics, conveyed inside the heated barrel and after partial melting, injected into the mold cavity to form net-shape product.^[1] In this process, the solid-state deformation is the principal mechanism controlling the feedstock melting and is critical for generation of thixotropic structures.^[34] The role of feedstock deformation was not acknowledged in original inventions of magnesium injection molding and

related early literature, where an action of injection screw was seen as the only factor controlling the feedstock transformation during heating. The later research within the manufacturing industry of injection molding machinery revealed the very detailed structure of the particulate feedstock and its transformation characteristics during heating into semisolid state.^[1,36]

C. Powder Thixoforming

There are also reported thixoforming experiments with powder particulates as solid precursors. In powder thixoforming, green billets are first obtained by blending and cold pressing a powder mixture, which is then partially melted and thixoformed.^[188] When using a mixture of Ti and Al alloy powders, cold pressing and partial melting the Al_3Ti reinforcing particles were generated in the Al_3Ti_p/Al matrix composites.^[189] The same technique of powder thixoforming was used to manufacture the core-shell-structured $(Al, Si)_3Ti_p$ particulate-reinforced A356 composites.^[190]

It appears that there is no full analogy between partial melting behavior of powders and coarse particulates described above. In case of powder, the primary particle size in semisolid slurry equals to several diameters of the original powder, so it is different from coarse particulates forming numerous clusters of grains within a single chip.

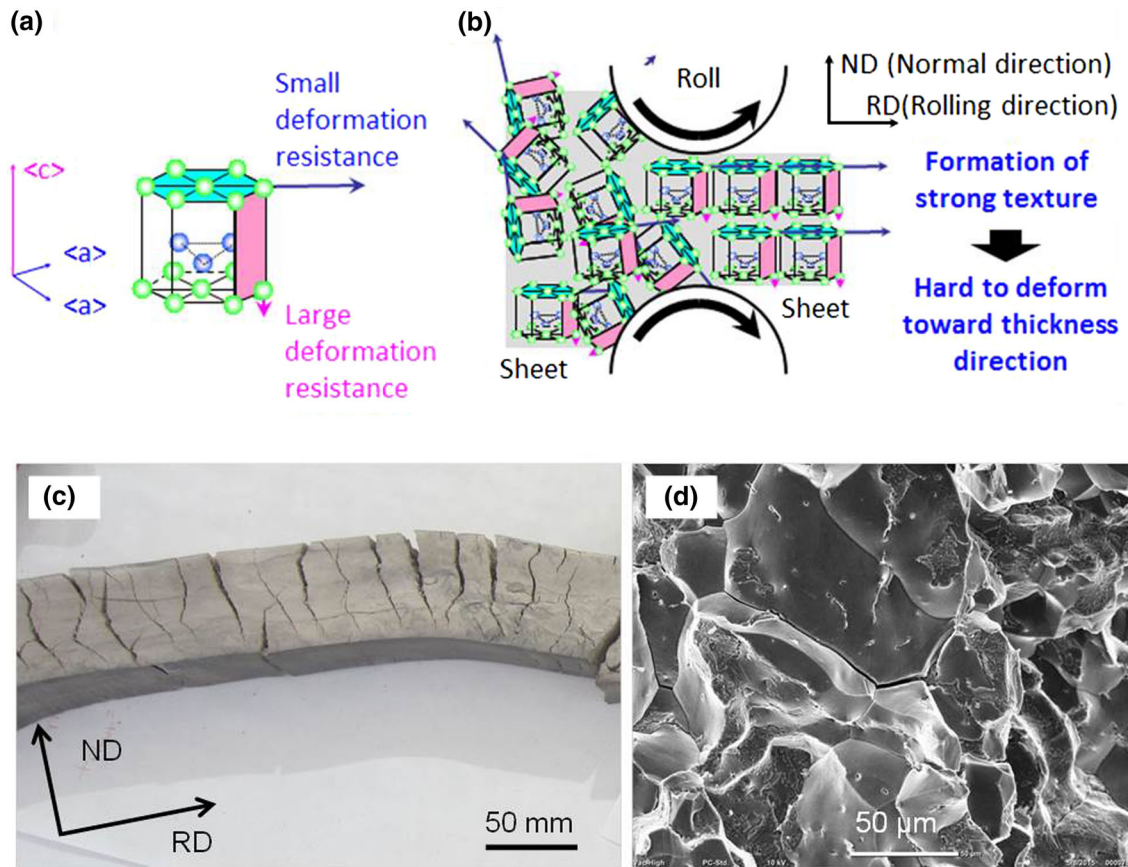


Fig. 29—Explaining low formability of magnesium: (a) anisotropy of magnesium crystal at room temperature; (b) texture formation during rolling process; (c) cracking of magnesium alloys during attempts of rolling; (d) brittle fracture surface of magnesium alloy cracked during rolling. Reprinted from Ref. [258].

IX. LABORATORY AND INDUSTRIAL IMPLEMENTATIONS

Thermomechanical processing of feedstock for thixoforming is used mainly at the laboratory but also at industrial scale. Still limited examples of fully commercial use are listed in References 37, 58 and 191. The deformation patterns cover single, two-step and multistep treatments involving hot and/or cold working. The key differences are associated with techniques of imposing deformation. There is a limitation on the billet size that is possible to prepare through solid-state deformation and typical dimensions are usually too small for many industrial components.

A. Extrusion

The majority of alloys processed by extrusion include both cast and wrought aluminum grades. There are findings showing that extrusion parameters affect the billet quality and properties of thixoformed components. This fact was revealed for billets of the A356 aluminum alloy fabricated by a hot extrusion through a flat-face and a curved die.^[192] In the case of extrusion *via* the flat-face die, there was a large variation in the average grain size and the mean roundness of equiaxed α -Al grains accompanied by a large scattering in the tensile properties throughout the part. In contrast, when

the billet extruded through the curved die was used as the feedstock, limited variation in tensile properties was observed.

The warm extrusion was found effective in generating a uniform and spheroidal microstructure suitable for thixoforming in the AA7005 aluminum alloy.^[193] After thixoforming at 605 °C and T6 heat treatment, the highest tensile properties reached 237 MPa, 361 MPa, and 16.8 pct for yield stress, ultimate tensile strength, and elongation, respectively. It was found that more liquid fraction at the temperature of 612 °C is beneficial for homogeneity of solid distribution within the thixoformed part. Similarly, hot extrusion was effective in billet manufacturing of the AA6061 aluminum alloy. The extrusion of the as-cast alloy in a hydraulic press at 460 °C with an extrusion ratio of 14:1 followed by partial melting at 635 °C for 5 minutes led to solid particle diameter of 100 μm .^[194] The globule/matrix interfaces were harder than the Al matrix itself. The deformation method by hot extrusion with a ratio of 27:1 was used with the same AA6061 aluminum alloy to disintegrate the initial dendritic structure for thixoforming.^[17] After partial melting, Cu, Mg, and Si were the major elements distributed along the globule/matrix interfaces. Also, the single-step hot extrusion was used to deform the AA6066 Al-Mg-Si alloy leading to fine, globular, and uniform morphology after a

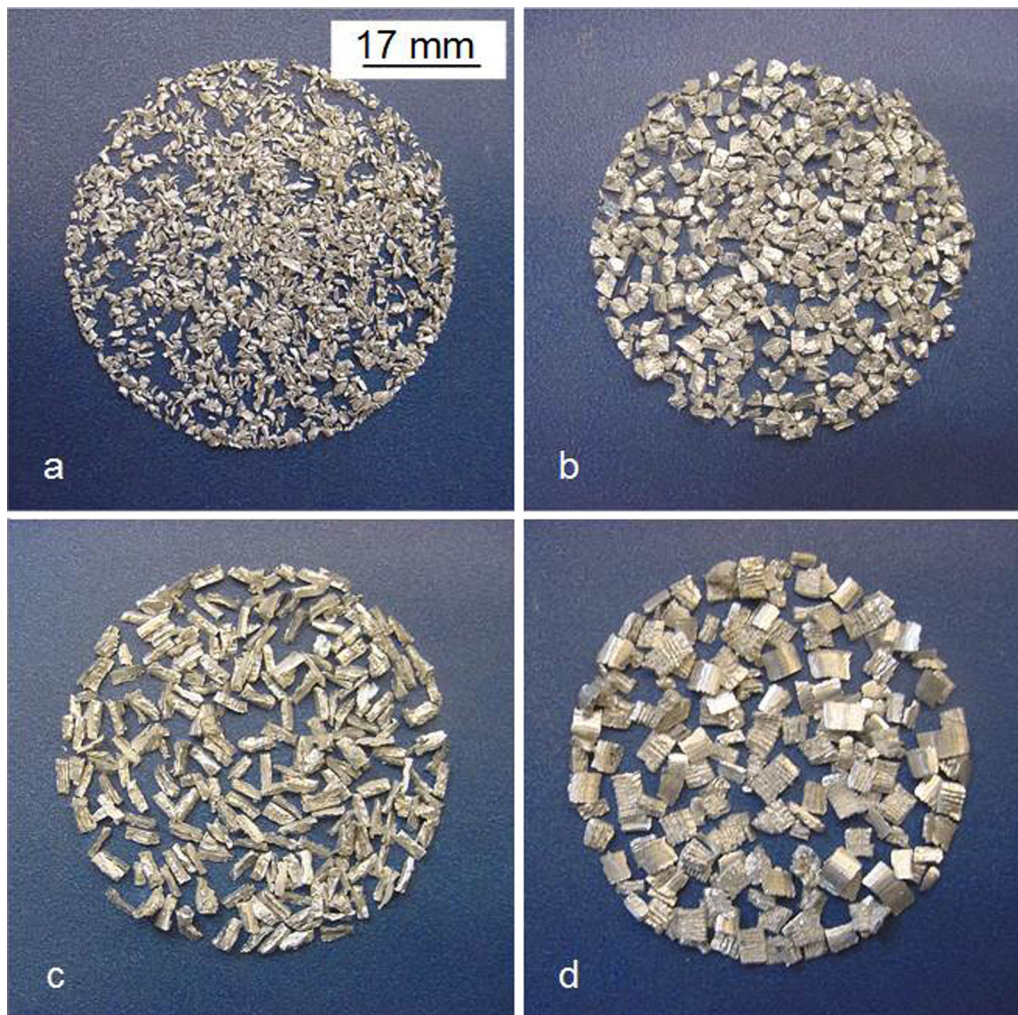


Fig. 30—Examples of chips manufactured by mechanical comminuting: (a) ZA27 zinc alloy; (b) AZ91D magnesium alloy—cutting followed by grinding; (c) AZ91D—cutting only; (d) MEZ magnesium alloy with additions of rare earth elements—turning. Reprinted with permission from Ref. [253].

short-duration salt bath treatment.^[18] With increasing the extrusion ratio, the dynamic recrystallization became more severe producing smaller recrystallized grain.

A single-step hot extrusion at 330 °C to 350 °C was found to be effective for the AZ61 magnesium alloy.^[13] The directly cast bars with a diameter of 203 mm (8.5 in.) were extruded to diameter of 76 mm (3 in.), heated to a semisolid state and formed by squeeze casting. In the case of the AZ80 alloy modified with micro additions of Y, a single-step extrusion was effective during billet preparation for thixoforming.^[159]

B. Compression

A cold compression with a reduction in height by up to 40 pct was used for the AA7075 aluminum alloy.^[195] After heating to semisolid range of 625 °C, the average size of solid particles gradually decreased with the increasing compression ratio, and the largest reductions

were seen for compressions below 30 pct. An uniaxial compression of 10 to 40 pct at ambient temperature was sufficient to generate globular particles in the Al-Zn-In alloy.^[22] Increasing the compression ratio from 10 to 30 pct, positively affected the particle sphericity after isothermal holding between 635 °C and 660 °C for 40 minutes. Further increasing the compression ratio up to 40 pct led to particle coarsening and reduction in their sphericity. The same compression range of 28 to 30 pct at 300 °C was also effective for the AZ31B magnesium alloy.^[160]

A requirement of minimum deformation to generate globular morphologies was demonstrated on high-melting point, high-entropy alloy AlCoCrCuNi.^[196] As shown in Figure 32, compression deformation at 850 °C with a strain of 25 pct did not generate globular forms after partial melting as was the case after larger deformation of 50 pct imposed at 1050 °C. It seems also that for the AM60B alloy the compression extend affected the microstructure after partial melting.^[197] The

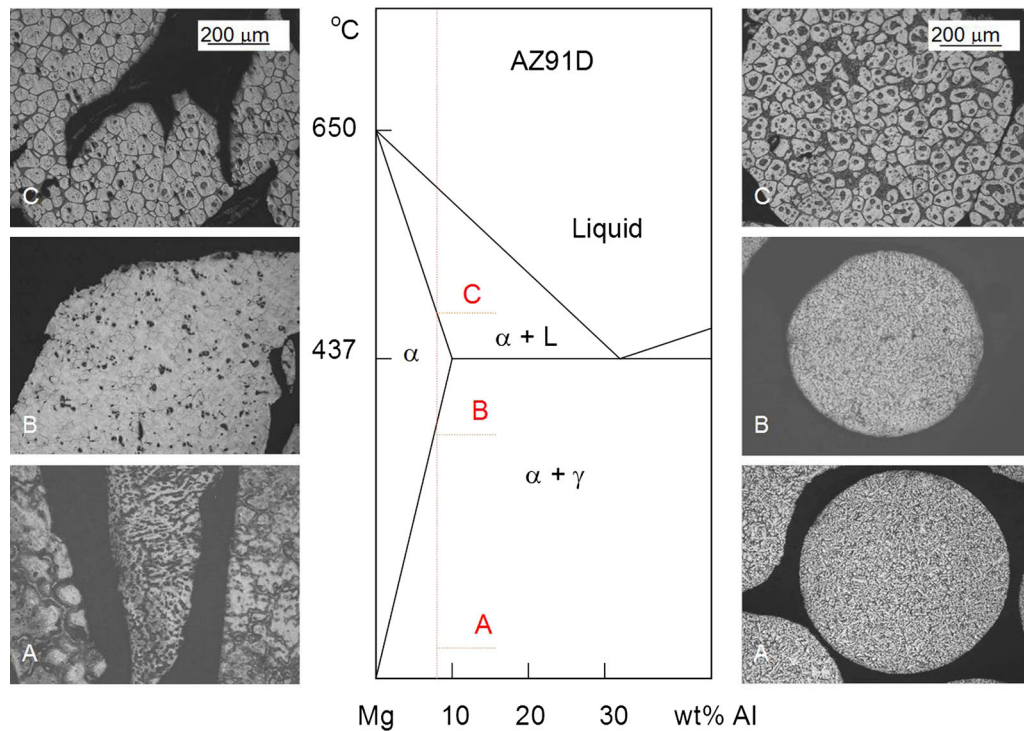


Fig. 31—Microstructure transformations within Mg-9Al-1Zn chips produced by mechanical comminuting (left hand side) and granules produced by rapid solidification (right hand side) during heating. The corresponding temperatures are indicated on simplified phase diagram: *A* room temperature, *B* heated in solid state above recrystallization temperature, *C* heated into semisolid state. Reprinted with permission from Ref. [185].

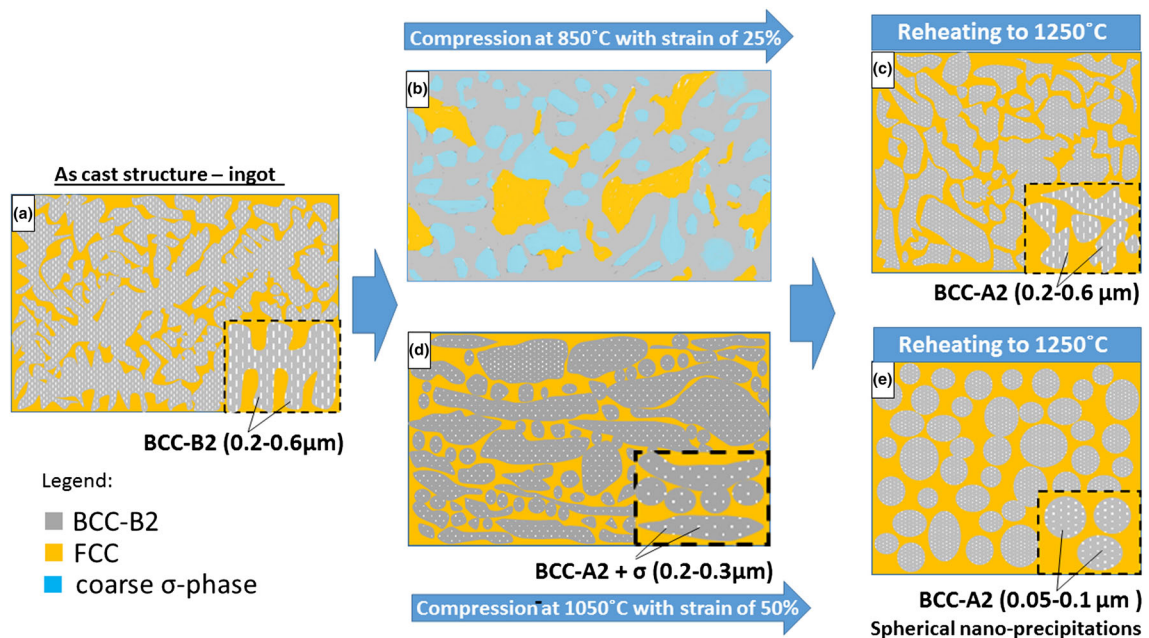


Fig. 32—Schematic illustration of the microstructural evolution of cast AlCoCrCuNi high-entropy alloy (*a*) after deformation of 25 pct strain rate at 850 °C (*b*) followed by partial melting at 1250 °C (*c*) and 50 pct strain rate at 1050 °C (*d*) followed by partial melting at 1250 °C (*e*). Only in the case (*d*), the partial melting led to a spheroidal morphology. Reprinted with permission from Ref. [196].

coarse-grained structure disappeared and a fine-grained structure resulted in the cyclic extrusion compressed alloy. However, coarse grains and recrystallized grains co-existed when the same alloy was deformed by

conventional compression. After partial melting, the alloy treated by cyclic extrusion compression exhibited fine microstructure, in which spheroidal solid particles contained pools of entrapped liquid.

C. Rolling

A possibility of utilizing ultra high strain hot rolling, consisting of one rolling pass with large thickness reductions was examined for grain refinement in the AZ91 alloy.^[198] The large deformation led to grain refinement and the dynamic recrystallization mechanism was highly dependent of the initial texture. The process is seen as an alternative to other more expensive deformation methods such as powder metallurgy or ECAE. The conventional rolling was effective to manufacture semisolid billet of the ZCuSn10 (88.25Cu, 10.48Sn) alloy.^[95] Two or four pass rolling after holding 15 minutes at 450 °C which led to 10 and 20 pct deformation was sufficient to generate globular morphologies after partial melting. For the wrought AA7075 aluminum alloy, rolling was found to be effective to eliminate a presence of continuous and brittle intermetallic compounds from grain boundaries as it was the case for conventional SIMA process.^[20]

D. Forging

Experiments with the A356 alloy showed that radial forging can induce enough strain at 60 pct of area reduction to prepare billet for high solid fraction thixoforming.^[199] Similarly, as it was observed for other deformation techniques, further increasing reduction up to 75 pct did not contribute to the microstructure improvement. Radial forging at the temperature of 300 °C was also used to deform the AA6063 Al alloy bar into a stepped shaft with different area reduction ratios.^[172] An isothermal holding in solidus–liquidus range showed that increasing deformation ratio led to smaller grain size and improved sphericity. For the AA7175 Al alloy, an improvement was recorded for the modified processing consisting of casting, two-stage homogenization, warm multiforging, recrystallization followed by semisolid forming, compared with multistage conventional process consisting of casting, hot working, and cold rolling with a reduction ratio up to 20 pct.^[16] The improved efficiency of the modified process was attributed to the enhanced recrystallization kinetics due to the relatively large amount of uniform deformation imposed by multiforging and a high density of Mg(Zn, Al, Cu)₂ precipitates. It is believed that precipitates, formed by two stage homogenization, acted as the preferential recrystallization sites.

Upsetting at 300 °C at a constant strain rate of 1/s with 25 and 50 pct cross-section reductions using a multistage hot-compression testing machine was effective to prepare a billet from the as-cast Cr-V-Mo steel (AISI H13).^[200] As a result, fine spherical structure with homogeneous distribution of carbides was generated. Larger deformations of 50 pct, higher heating rate of 50 °C/s and shorter holding time of 20 seconds were more effective in microstructure refinement through higher degree of nucleation during recrystallization, inhibiting the growth of austenite grains and coarsening of solid particles in solidus liquidus range.

For some alloys there is a possibility of improving properties created after thixoforming through heat treatment.^[201,202] In the case of H13 steel, the microstructural evolution caused by tempering

improved ductility. When tempering temperature was 560 °C, a good combination of mechanical properties was achieved. Schematic illustration of complex evolution of spheroidal microstructure during tempering at various temperatures is shown in Figure 33.

E. Severe Plastic Deformation

An application of the ECAE technique to manufacture billets for thixoforming was investigated for a variety of magnesium alloys including the AZ80,^[203] AZ91,^[25,153,204] ZW21,^[205] AM60,^[206] AM50^[207] and ZW61^[208] grades. The common benefit quoted is that the fine grain microstructure after deformation transforms to small granules in semisolid state. For the AZ91D alloy, the four-pass ECAE deformation at 300 °C resulted in an average grain size of 20 μm and after partial melting the globule size of 25 μm.^[204] For the same AZ91D alloy deformed by two pass ECAE at 280 °C after partial melting at 540 °C solid particles reached 50 μm.^[25] The tensile properties of the AM50, thixoformed alloy at 600 °C using a billet prepared by ECAE were roughly 30 pct higher than after forming at the same temperature of 600 °C using a cast billet.^[207] A finer microstructure was obtained for the same AZ91D alloy thixoformed after RUE at 285 °C, 310 °C, and 340 °C where solid particles reached 12 to 24 μm.^[209] For the ZK60 + RE alloy, the solid particle size was also smaller after ECAE at 350 °C using a die with curvature angle of the outside corner of 90 deg than after compression at 350 °C in a hydraulic press with the compression ratio of 40 pct.^[210] The solid particles in the slurry obtained after single-pass MDF of the A356 aluminum alloy developed a similar sphericity but smaller globule size than after MHD stirring.^[211] As reported for conventional deformation techniques, increasing the number of forging passes led to the coarsening of solid particles.

F. Combinations of Different Deformation Techniques

The comparison of combination of ECAE and hot rolling over a single deformation *via* hot rolling was documented for the Mg-3Zn cast magnesium alloy with α-Mg dendrites having an average secondary arm spacing of 250 μm.^[70] The single-step hot rolling at 350 °C refined the alloy microstructure by creating deformation bands of the α-Mg particles of the order of 10 to 50 μm that were separated by Zn-rich precipitates. Reheating led to globular morphology and at 630 °C, globular particles reached a diameter of 82 μm. An additional deformation of the hot-rolled alloy using the ECAP method at 250 °C led to laths with a thickness of 0.4 μm and a length of 3 μm as well as equiaxed grains with a diameter of 0.5 μm, both separated by Zn-rich precipitates. After reheating of this microstructure to a temperature of 630 °C, the spheroidal morphologies with an average globule size of 62 μm were formed. Thus, a step of ECAE deformation reduced solid globules by 25 pct compared to that achieved for hot-rolled billet (Figure 34). A similar globule size was obtained for extrusion of the AZ91 alloy at 350 °C to

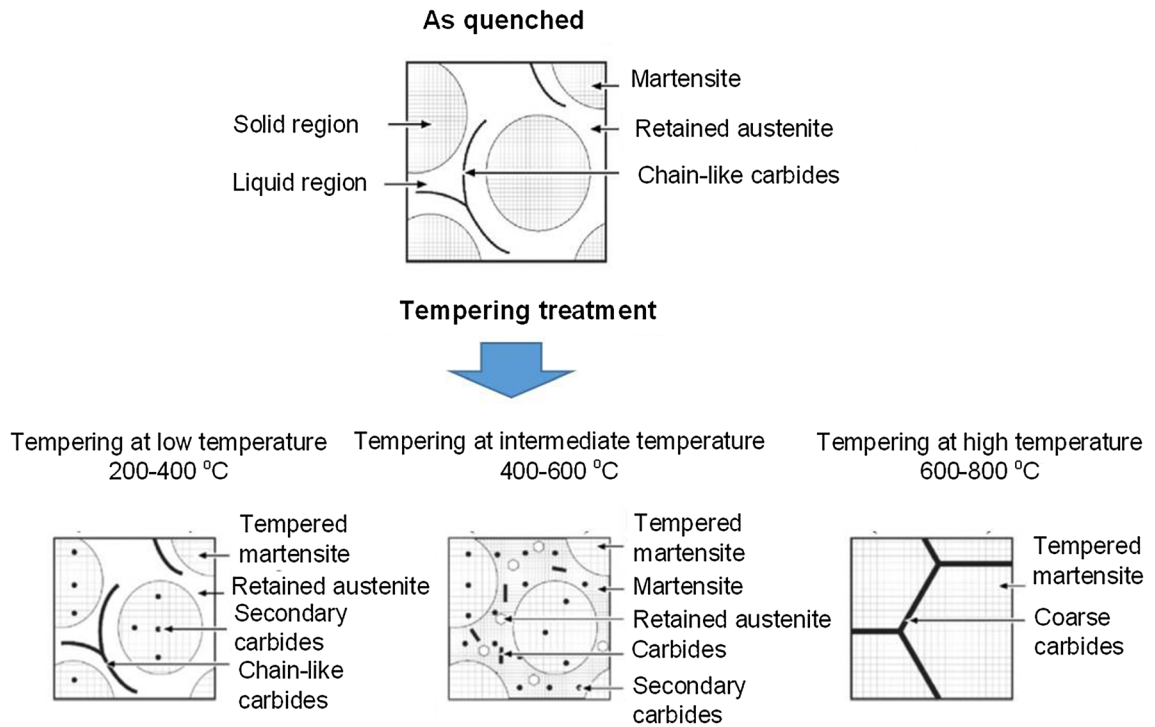


Fig. 33—Schematic illustration of microstructural evolution during tempering at various temperatures of thixoformed AISI H13 steel. Reprinted with permission from Ref. [202].

400 °C with a ratio of 30 to 50:1 followed by compression at 200 °C to 220 °C with a nominal strain of 20 to 40 pct.^[15] After isothermal holding at 570 °C to 580 °C for 30 to 180 seconds, the globular solid particles reached size in the range of 40 to 60 μm.

Majority of multistage treatments, however, do not provide assessments of individual steps, just focusing on the final effect. A combination of hot extrusion, solution treatment, aging, and upsetting with different ram velocities was conducted at temperature range of 280 °C to 380 °C of the LY11 aluminum alloy (4.1Cu, 0.64Mg, 0.54Mn with solidus of 514 °C and liquidus of 642 °C) revealed processing parameters affecting transformation into globular forms.^[212] After partial melting at 580 °C to 620 °C, the average size of grains increased with the increasing deformation temperature, and decreased with decrease in the ram velocity. Increasing the isothermal temperature and elongating holding time would benefit the fragmentation spheroidization and coarsening of solid particles. Similar behaviors were researched during forging and lateral extrusion of various aluminum alloys including grades designed for wrought processing.^[213]

G. Deformation in Semisolid State

Development of thixotropic structures by imposing deformation in semisolid state is beyond the scope of this review. The technique is briefly mentioned here since in the literature for its scenario the same SIMA term is sometimes used.^[30] For example, severe plastic deformation ECAP explored pressing the A356 aluminum alloy at 572 °C through two channels with an intersection angle of 90 deg.^[31] Then, the deformed material was subjected to

isothermal holding at the same temperature of 572 °C. As a result of the ECAP deformation and isothermal holding in the semisolid state, the fine spheroidal solid structure was created. It was concluded that the globular structure was observed even in early stages of the isothermal holding, the dendritic structure has completely broken down, and isothermal coarsening in the deformed alloys well obeys the LSW equation.

As expected, deformation of semisolid slurry involves different mechanisms than discussed in this report for solid-state SIMA. To identify these mechanisms, thixotropic compression test was conducted on a RUE-processed AZ91D magnesium alloy at temperatures ranging from 500 °C to 550 °C by means of a Gleeble-1500 thermal-mechanical simulator.^[29] Among deformations experienced by the slurry, the elastic-like deformation, strain-hardening deformation, and rheological viscoplastic deformation were named. The dominant deformation mechanisms included slipping or rotating mechanism of the solid particles along the liquid films, the slipping mechanism between the solid particles, the plastic deformation mechanism of the solid particles, and the dynamic recrystallization within solid particles.

X. AN ASSESSMENT MATRIX FOR THIXOFORMING

For a manufacturing technology to achieve the commercial acceptance in today's market, clear advantages of superior product properties and competitive cost must be demonstrated. Unfortunately, when assessing the advantages of semisolid routes over conventional

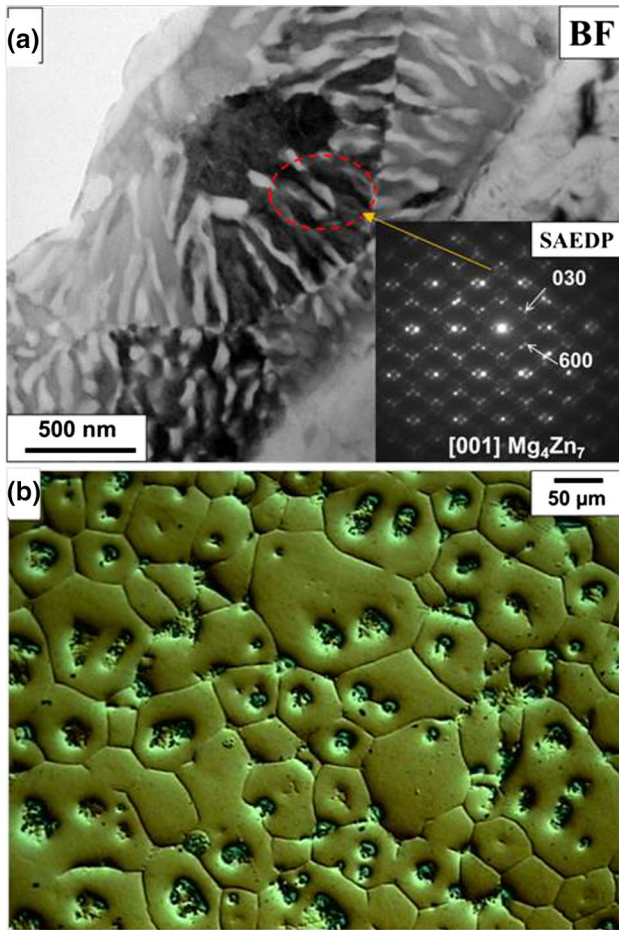


Fig. 34—Microstructure of the Mg-3 pct Zn alloy after hot rolling, ECAP deformation followed by reheating to 630 °C and water quench: (a) TEM micrograph of the grain boundary region and diffraction pattern with indexation of reflections from the area marked by red ring; (b) optical image after etching, observed in bias light. Reprinted from Ref. [70] (Color figure online).

techniques such a single evident advantage often does not exist. Therefore, to understand differences between conventional and novel processing techniques, an assessment matrix should be created. An example of processing elements to be considered during such a comparison is shown in Table III.

For thixoforming the assessment is not straightforward since some factors may superimpose on each other. For example, while comparing mechanical properties it is difficult to separate the contribution of porosity and other defects in casting from the microstructural factor.

A change of manufacturing from casting to thixoforming and then to wrought processing is associated with a transition from dendrites to globular morphologies to equiaxed grains. These changes are superimposed on a reduction in porosity and other defects related to melt solidification. Then, the same is valid for a comparison between semisolid microstructures generated at different temperatures. The lower thixocasting temperature, the lower contribution of liquid and associated with it solidification shrinkage and other melt-related defects. At the same time, the higher contribution of globular forms that replace dendritic morphologies. It is a common expectation that reduced temperature will lead to better properties. So far, there is no consistent evidence that the microstructure of present alloys, generated after semisolid processing, leads to substantial increase in mechanical properties with reduced processing temperature. In fact, for magnesium alloys, there are examples showing exactly the opposite trend.^[141]

There should also be a distinguished difference between properties of an alloy manufactured as a test sample and properties of the same alloy within different regions of a net-shape component. The intricate shape of components will influence defect formation during manufacturing with a contribution from liquid fraction. The properties after thixoforming are usually located between values generated after casting and after wrought processing. To show the scale of differences, several selected examples are listed in Table IV. Some additional results may be found in Reference 214. It is seen that for thixoforming of cast alloys tensile properties exceed their equivalents achieved after casting. However, the properties of wrought alloys after thixocasting are generally below values obtained after wrought processing. The misleading conclusions are sometimes reached in the literature by utilizing the hot-worked state as a comparison base for wrought alloys. One should, however, remember that the optimal properties of wrought alloys are not those achieved after hot rolling or hot extrusion.

XI. CONCLUDING REMARKS

Thermomechanical treatment of cast solid metals prior to partial melting represents an effective tool of influencing the solidification outcome and converting dendritic structures into globular morphologies. The concept is explored for manufacturing billets for thixoforming using a variety of alloys ranging from low

Table III. An Example of Matrix Used for Assessing the Semisolid Processing

	Casting	Semisolid Processing	Wrought Processing
Major Structural Features	dendrites	globules/dendrites	grains
Internal Integrity (Porosity-P)	P_c	$P_{ssp} < P_c$	0
Alloy Properties	low	intermediate	high
Component Properties	low	intermediate	high
Heat Treatment Capabilities	no/yes	yes/no	yes
Process Temperature	above liquidus	liquidus–solidus	below solidus
Relative Component cost	low	intermediate/high	high

Table IV. Tensile Properties of Selected Alloys Manufactured by Semisolid Metal Processing with Exploring SIMA Prepared Billets

Alloys	Designation	Cast/ Wrought	Semisolid Processing				Conventional Processing				References	
			Billet Preparation Route	SIMA	UTS (MPa)	YS (MPa)	El. (Pct)	Process	UTS (MPa)	YS (MPa)		El. (Pct)
AM50		cast	ECAE		312	183	14	thixoforming of the as-cast billet	245	127	9	207
AZ91D		cast	ECAE		328.9	203.8	16.1	HPDC	240	165	3	153, 249
AZ91D		cast	upsetting		253.4	168.9	7.8					153
AZ80		wrought	ECAE		≈ 310	≈ 250	≈ 20	forged	330	230	12	1, 203
Mg-8.5Gd-3.72Y-0.54Zr		cast	extrusion		208	162	5.4	permanent mold casting	187	155	1.2	26
SKD61 (SAE H13) Steel		wrought	cast, compression, T6*		1450	632	18.8	forged T6*	1835	1530	13	200, 202,
AA7075		wrought	cast, RAP, 50 pct deformation		585	432	17.5	hot-rolled	574	302	30	250
A356		wrought cast	commercially extruded rolling, forging		220 212	145	5.1 14.6	extruded permanent mold cast	398 530 180	145 90	2.2 9.7 3.0	251 252

UTS: tensile strength, YS: yield stress, El.: elongation.
*Data after T6 heat treatment with tempering at 560 °C.

temperature melting aluminum and magnesium to steel and Co based grades. The solid-state deformation is also essential for coarse particulate feedstock, utilized for semisolid forming either directly or after compaction into billets. Although the original deformation concept, called SIMA, defined the specific procedure, the term became a generally recognized synonym for a variety of thermomechanical treatments offering an opportunity of controlling the solidification microstructure. It is generally accepted that the solid-state deformation treatment provides high-quality billets for thixoforming, but it represents additional steps in manufacturing cycle, increasing substantially the component cost. Although the complex, frequently multiple deformation scenarios, ranging from conventional to severe plastic deformation techniques, generate very fine-grained structures in the billet, there is no evidence that the extra manufacturing efforts are fully compensated by a corresponding increase in properties of a thixoformed component to the level that allows it to successfully compete with well-established conventional technologies of mass-scale production.

REFERENCES

1. F. Czerwinski: *Magnesium Injection Molding*, Springer, New York, 2008.
2. E. Vinarcik: *High Integrity Die Casting Processes*, Wiley, New York, 2003.
3. D. Spencer, R. Mehrabian, and M. Flemings: *Metall. Trans.*, 1972, vol. 3, pp. 1925–32.
4. A. Kopper: SoD, slurry-on-demand, casting method and charge. US Patent Application 20080060779 A1, 13 March 2008.
5. M. Schwartz, ed.: *Innovations in Materials Manufacturing, Fabrication, and Environmental Safety*, CRC Press, Boca Raton, FL, 2011.
6. G. Hirt, R. Cremer, T. Witulski, and H. Tinius: *Mater. Des.*, 1997, vol. 18, pp. 315–21.
7. N. Husain, A. Ahmad, and M. Rashidi: *IOP Conf. Ser. Mater. Sci. Eng.*, 2017, vol. 257, p. 012053. <https://doi.org/10.1088/1757-899x/257/1/012053>.
8. M. Rosso: *J. Achiev. Mater. Manuf. Eng.*, 2012, vol. 54, p. 9.
9. F. Czerwinski: *Adv. Mater. Process.*, 2016, vol. 174, pp. 19–22.
10. F. Czerwinski: *Metall. Mater. Trans. B*, 2017, vol. 48B, pp. 367–93.
11. K.P. Young, C.P. Kyonka, and J.A. Courtois: Fine grained metal composition. US Patent 4,415,374, 15 Nov 1983.
12. D. Kirkwood, C. Sellars, and L. Elias Boyed: Thixotropic materials. US Patent 5,133,811, 28 July 1992.
13. G. Woodhouse: Semi-solid metal forming process. Patent WO1998033610A1, 31 Jan 1997.
14. G. Woodhouse: Semi-solid metal forming process. US Patent 6,079,477, 27 June 2000.
15. S. Park: Method for fabricating magnesium alloy billets for thixoforming process. US Patent 7,083,689 B2, 1 Aug 2006.
16. Y. Song, K. Park, and C. Hong: *Mater. Trans.*, 2006, vol. 47, pp. 1250–56.
17. C. Lin, F. Hung, and T. Lui: *Metals*, 2016, vol. 183, pp. 1–12.
18. C. Lin, F. Hung, T. Lui, and L. Chen: *Metals*, 2016, vol. 6, pp. 1–13.
19. C. Lin, F. Hung, and T. Lui: *Mater. Sci. Eng. A*, 2016, vol. 659, pp. 143–57.
20. M. Karamouz, M. Alizadeh, and A. Ahmadi: Preprints, 2017. <https://doi.org/10.20944/preprints201704.0172.v1>.
21. M. Karamouz, M. Alzadeh, and A. Ahmadi: *Int. J. Mater. Res.*, 2017, vol. 108, pp. 1073–80.

22. B. Shayegh-Boroujeny, M. Ghashghaei, and E. Akbari: *J. Alloys Compd.*, 2018, vol. 731, pp. 354–63.
23. Q. Zhang, Z. Cao, Y. Zhang, G. Su, and Y. Liu: *J. Mater. Process. Technol.*, 2007, vol. 184, pp. 195–200.
24. Q. Zhang, Z. Cao, Y. Liu, Y. Zhang, L. Zhang, M. Zhang, and R. Wu: *Mater. Sci. Eng. A*, 2008, vol. 488, pp. 260–65.
25. S. Luo, Q. Chen, and Z. Zhao: *J. Alloys Compd.*, 2009, vol. 477, pp. 602–07.
26. L. Gao, R. Chen, and E. Han: *Mater. Sci. Technol.*, 2011, vol. 27, pp. 1084–91.
27. Y. Zhou, J. Lu, N. Saluja, and A. Riviere: Processes for producing fine grained metal compositions using continuous extrusion for semisolid forming of shaped articles. US Patent 6,120,625, 19 Sep 2000.
28. B. Binesh and M. Aghaie-Khafri: *Mater. Des.*, 2016, vol. 95, pp. 268–86.
29. Y. Xu, C. Chen, J. Jia, X. Zhang, H. Dai, and Y. Yang: *J. Alloys Compd.*, 2018, vol. 748, pp. 694–705.
30. S. Hossein Nedjad, H. Meidani, and M. Nili Ahmadabadi: *Mater. Sci. Eng. A*, 2008, vol. 475, p. 224.
31. H. Meidani, S. Hossein-Nedjad, and M. Nili-Ahmadabadi: *Solid State Phenom.*, 2008, vols. 141–143, pp. 445–50.
32. P. Kapranos: in *Thixoforming Steel*, H. Atkinson and A. Rassili, eds., Shaker Verlag, Aachen, 2010, pp. 13–36.
33. K. Solek, L. Rogal, and P. Kapranos: *J. Mater. Eng. Perform.*, 2017, vol. 26, pp. 115–23.
34. F. Czerwinski: *Metall. Mater. Trans. A*, 2002, vol. 33A, pp. 2963–72.
35. F. Czerwinski and A. Zielinska-Lipiec: *Acta Mater.*, 2003, vol. 51, pp. 3319–32.
36. F. Czerwinski: *Acta Mater.*, 2002, vol. 50, pp. 3265–81.
37. G. Hirt and R. Kopp: *Thixoforming: Semi-solid Metal Processing*, Wiley VCH, Weinheim, 2009.
38. S. Nafisi and R. Ghomashchi: *Semi-solid Processing of Aluminum Alloys*, Springer, New York, 2016.
39. M. Flemings: *Metall. Trans.*, 1991, vol. 22A, pp. 957–81.
40. Z. Fan: *Int. Mater. Rev.*, 2002, vol. 47, pp. 49–85.
41. F. Czerwinski: *Mater. Sci. Eng. A*, 2005, vol. 392, pp. 51–56.
42. E. Schalek and A. Szegvari: *Kolloid. Z.*, 1923, vol. 32, p. 318.
43. T. Peterfi: *Arch. Entwickl. Organ.*, 1927, vol. 32, p. 680.
44. H. Barnes: *J. Non-Newton. Fluid Mech.*, 1997, vol. 70, pp. 1–33.
45. F. Czerwinski: *JOM*, 2006, vol. 57, pp. 17–20.
46. I.M. Krieger and T.J. Dougherty: *Trans. Soc. Rheol.*, 1959, vol. 3, p. 137.
47. M. Perez, J. Barbe, Z. Neda, Y. Brechet, and L. Salvo: *Acta Mater.*, 2000, vol. 48, pp. 3773–82.
48. D.J. Jeffrey and A. Acrivos: *AIChE J.*, 1976, vol. 22, p. 417.
49. S. Lind: *J. Phys. Chem.*, 1940, vol. 44 (6), pp. 829–829.
50. Ritwik: *Measuring the Viscous Flow Behaviour of Molten Metals Under Shear*. Brunel University, London, 2012.
51. R. Chhabra and J. Richardson: *Non-Newtonian Flow in the Process Industries*. Butterworth-Heinemann, Oxford, 1999.
52. L. Battezzati and A. Greer: *Acta Metall.*, 1989, vol. 37, pp. 1791–1802.
53. T. Liu, H. Atkinson, P. Kapranos, D. Kirkwood, and S. Hogg: *Metall. Mater. Trans. A*, 2003, vol. 34A, pp. 1545–54.
54. P. Kapranos, T. Liu, H. Atkinson, and D. Kirkwood: *J. Mater. Process. Technol.*, 2001, vol. 111, pp. 31–36.
55. S. Hogg, H. Atkinson, and P. Kapranos: *Metall. Mater. Trans. A*, 2004, vol. 35A, pp. 899–910.
56. S. Midson: *Die Cast. Eng.*, 2006, vol. 50 (1), p. 48.
57. D. Kirkwood, M. Suery, P. Kapranos, H. Atkinson, and K. Kenneth: *Semi-solid Processing of Alloys*, Springer, Berlin, 2009.
58. A. De Figueredo, ed.: *Science and Technology of Semi-Solid Metal Processing*, Worcester Polytechnic Institute, Worcester, MA, 2001.
59. F. Czerwinski and G. Birsan: *Metall. Mater. Trans. B*, 2017, vol. 48B, pp. 983–92.
60. M. Krivokorytov, Q. Zeng, B. Lakatos, A. Vinokhodov, A. Sidelnikov, and V. Kompanets: *Sci. Rep.*, 2018, vol. 8, p. 597.
61. Z. Xuan, F. Mao, Z. Cao, T. Wang, and L. Zou: *J. Alloys Compd.*, 2017, vol. 721, pp. 126–33.
62. F. Yang, Z. Chen, F. Cao, R. Fan, H. Kang, W. Huang, Q. Yuan, Y. Fu, and T. Wang: *J. Mater. Sci. Technol. (Shenyang China)*, 2017, vol. 33, pp. 1134–40.
63. V. Laxmanan: Process for manufacturing spheroidal hypoeutectic aluminum alloy. US Patent 5,009,844, 23 April 1991.
64. S. Wang and W. Jie: *Acta Mater.*, 2004, vol. 52, pp. 415–22.
65. S. Bergsma: Casting, thermal transforming and semi-solid forming aluminum alloys. US Patent 5,571,346, 5 Nov 1996.
66. T. Chen, Y. Ma, R. Wang, Y. Li, and Y. Hao: *Trans. Nonferr. Met. Soc. China*, 2010, vol. 20 (9), pp. 1615–21.
67. H. Wang, C. Davidson, and D. St John: *Mater. Sci. Eng. A*, 2004, vol. 368, pp. 159–67.
68. T. Chen, H. Zhao, Y. Ma, and Y. Hao: *Met. Mater. Int.*, 2005, vol. 11, pp. 513–20.
69. A. Pola, R. Roberti, and L. Montesano: *Int. J. Mater. Form.*, 2010, vol. 3, pp. 743–46.
70. L. Rogal, F. Czerwinski, L. Litynska-Dobrzynska, P. Bobrowski, A. Wierzbica-Miernik, and J. Dutkiewicz: *Solid State Phenom.*, 2015, vols. 217–218, pp. 381–88.
71. K. Solek and P. Kapranos: *Arch. Metall. Mater.*, 2016, vol. 61, pp. 1901–08.
72. L. Rogal, W. Solano-Alvarez, and H. Bhadeshia: *Mater. Sci. Technol.*, 2017, vol. 33, pp. 870–78.
73. L. Rogal: *Mater. Sci. Technol.*, 2017, vol. 33, pp. 759–64.
74. F. Czerwinski: *Acta Mater.*, 2002, vol. 50, pp. 2639–54.
75. F. Czerwinski: *Corros. Sci.*, 2014, vol. 86, pp. 1–16.
76. F. Czerwinski: *Int. Mater. Rev.*, 2015, vol. 50, pp. 264–96.
77. H. Nakato, M. Oka, S. Itoyama, M. Urata, T. Kawasaki, K. Hashiguchi, and S. Okano: *Mater. Trans.*, 2002, vol. 43, pp. 24–29.
78. L. Xie, J. Xu, B. Yang, Z. Zhang, and L. Shi: *Solid State Phenom.*, 2006, vols. 116–117, pp. 72–75.
79. E. Lavrnia and T. Srivatsan: *J. Mater. Sci.*, 2010, vol. 45, p. 287.
80. A.G. Leatham and A. Lawley: *Int. J. of Powder Met.*, 1993, vol. 29 (4), pp. 321–29.
81. F. Czerwinski: *Mater. Sci. Eng. A*, 2004, vol. 367, pp. 261–71.
82. J. Aguilar, M. Fehlbier, A. Ludwig, A. Buhning-Polaczek, and P. Sahn: *Mater. Sci. Eng. A*, 2004, vols. 375–377, pp. 651–55.
83. M. Fehlbier, J. Aguilar, and P. Sahn: *Int. J. Cast Met. Res.*, 2001, vol. 14, pp. 71–78.
84. E. Ogris: Development of Al-Si-Mg Alloys for Semi-solid. Ph.D. Thesis, Swiss Federal Institute of Technology, Zurich, 2002.
85. H. Xu, Z. Ji, M. Hu, and Z. Wang: *Trans. Nonferr. Met. Soc. China*, 2010, vol. 20, pp. s749–53.
86. H. Xu, Z. Ji, Y. Wang, M. Hu, H. Wang, and S. Sugiyama: *Solid State Phenom.*, 2016, vol. 256, pp. 45–50.
87. F. Kido and T. Motegi: *Mater. Sci. Forum*, 2009, vols. 610–613, pp. 1403–06.
88. H. Xu, Z. Ji, and Z. Wang: *Solid State Phenom.*, 2013, vols. 192–193, pp. 238–45.
89. G. Dieter: *Mechanical Metallurgy*, McGraw-Hill, New York, 1976.
90. E. Mittemeijer: *Fundamentals of Materials Science*, Springer, Berlin, 2011, pp. 463–96.
91. E. Hornbogen and U. Koster: *Recrystallization of Metallic Materials*, Dr. Riederer-Verlag, GmbH, Stuttgart, 1978, pp. 159–94.
92. A. Bhaduri: *Mechanical Properties and Working of Metals and Alloys*, Springer, Berlin, 2018.
93. F. Musin, A. Belyakov, R. Kaibyshev, Y. Motohashi, G. Itoh, and K. Tsuzaki: *Rev. Adv. Mater. Sci.*, 2010, vol. 25, pp. 107–12.
94. T. Sakai, A. Belyakov, R. Kaibyshev, H. Miura, and J. Jonas: *Prog. Mater. Sci.*, 2014, vol. 60, pp. 130–207.
95. J. Wang, D. Lu, H. Xiao, F. Zhou, R. Zhou, and L. Wu: *Solid State Phenom.*, 2015, vols. 217–218, pp. 418–25.
96. R. Kamachali: Grain Boundary Motion in Polycrystalline Materials. Ph.D. Thesis, Ruhr-Universität Bochum (RUB), Bochum, 2012.
97. M. Hillert: *Acta Metall.*, 1965, vol. 13, pp. 227–38.
98. N. Loiat and M. Duesbery: *Philos. Mag. A*, 1994, vol. 69, pp. 841–54.
99. M. Bauser, G. Sauer, and K. Siebert: *Extrusion*, ASM International, Materials Park, OH, 2006.
100. J. Ajiboy and M. Adeyemi: *J. Mech. Sci. Technol.*, 2007, vol. 21, p. 1553.
101. Swaging: Rotary and Extrusion, EngineeringClicks, 08 09 2017. <https://www.engineeringclicks.com/rotary-swaging-extrusion-swaging/>. Accessed 10/5/2018.

102. M. Furukawa, Z. Horita, M. Nemoto, and T. Langdon: *J. Mater. Sci.*, 2001, vol. 36, pp. 2835–43.
103. R. Valiev: *Mater. Sci. Eng. A*, 1997, vol. 59, pp. 234–36.
104. M. Aliofkhaezrai and B. Ravisankar: *Handbook of Mechanical Nanostructuring*, Wiley-VCH Verlag GmbH and Co. KGaA, 2015. <https://doi.org/10.1002/9783527674947>.
105. V. Varyukhin, Y. Betgelzimer, R. Kulagin, O. Prokofeva, and A. Reshetov: *Mater. Sci. Forum*, 2011, vols. 667–669, pp. 31–37.
106. R. Pippan, S. Scheriau, A. Hohenwater, and M. Hafok: *Mater. Sci. Forum*, 2008, vols. 584–586, pp. 16–21.
107. R. Valiev, R. Ilsamgaliev, and I. Alexandrov: *Prog. Mater. Sci.*, 2000, vol. 45, p. 101.
108. P. Bridgman: *Phys. Rev.*, 1935, vol. 48, pp. 825–47.
109. G. Salishchev, O. Valiakhetov, and R. Galeyev: *J. Mater. Sci.*, 1993, vol. 28, pp. 2898–2902.
110. L. Zaharia, R. Comaneci, R. Chelariu, and D. Luca: *Mater. Sci. Eng. A*, 2014, vol. 595, pp. 135–42.
111. W. Tang, R. Chen, J. Zhou, and E. Han: *Mater. Sci. Eng. A*, 2009, vol. 499, pp. 404–10.
112. M. Afifi, Y. Wang, P. Pereira, Y. Wang, S. Li, Y. Huang, and T. Langdon: *Mater. Sci. Eng. A*, 2018, vol. 712, pp. 146–56.
113. X. Yang, H. Miura, and T. Sakai: *Mater. Trans.*, 2002, vol. 43, pp. 2400–07.
114. P. Bazarnik, B. Romelczyk, M. Kulczyk, and M. Lewandowska: *Mater. Sci. Forum*, 2013, vol. 765, pp. 423–28.
115. R. Comaneci, L. Zaharia, and D. Nedelcu: *Indian J. Eng. Mater. Sci.*, 2015, vol. 22, pp. 527–33.
116. C. Rentenberger and H. Karnthaler: *Acta Mater.*, 2005, vol. 53, pp. 3031–40.
117. A. Ishmaku and K. Han: *J. Mater. Sci.*, 2004, vol. 39, pp. 5417–20.
118. W. Xu, K. Kim, J. Das, and J. Eckert: *Appl. Phys. Lett.*, 2006, vol. 89. <https://doi.org/10.1063/1.2222239>.
119. A. Blatter and M. von Allmen: *Mater. Sci. Eng.*, 1988, vol. 97, pp. 93–95.
120. S. Han, L. Zhao, Q. Jiang, and J. Lian: *Sci. Rep.*, 2012, vol. 493. <https://doi.org/10.1038/srep00493>.
121. M. Liu: *Mater. Sci. Forum*, 2015, vol. 817, pp. 627–33.
122. X. Wu, N. Tao, Y. Hong, J. Lu, and K. Lu: *J. Phys. D*, 2005, vol. 38, p. 4140.
123. R. Hebert and J. Perepezko: *Mater. Res. Soc. Symp. Proc.*, 2003, vol. 740, pp. 267–72.
124. G. Wilde, H. Sieber, and J. Perepezko: *Scripta Mater.*, 1999, vol. 40, p. 779.
125. A. Kundu and A. Reynolds: Abnormal Grain Growth of AA2195 Friction Stir Weld Nugget during Solution Heat Treatment. Master Thesis, University of South Carolina, 2010.
126. J. Mohallem, J. Martins, C. Martins, and M. Machado: *Rev. Esc. Minas*, 2015, vol. 4, p. 68. <https://doi.org/10.1590/0370-44672014680140>.
127. X. Zhao, M. Niinomi, M. Nakai, and J. Hieda: *Mater. Trans.*, 2012, vol. 53, pp. 1379–84.
128. H. Kim, S. Lim, I. Yeo, and W. Kim: *Mater. Sci. Eng. A*, 2007, vols. 449–451, pp. 322–25.
129. J. Lewis: Formation of Deformation Induced Ferrite During Mechanical Testing. Master Thesis, McGill University, Montreal, 1996.
130. J. Liu: Deformation Induced Martensitic Transformation in 304 Stainless Steel. Master Thesis, University of South Carolina, 2016.
131. S. Pauly, J. Das, J. Bednarcik, N. Mattern, K. Kim, D. Kim, and J. Eckert: *Scripta Mater.*, 2009, vol. 60, pp. 431–34.
132. V. Levitas, B. Henson, L. Smilowitz, and B. Asay: *J. Phys. Chem. B*, 2006, vol. 110, pp. 10105–19.
133. NETZSCH Thermal Analysis. www.netzsch-thermal-analysis.com. Accessed 3/3/2018.
134. J. Sokolowski, W. Kierkus, M. Kasprzak, and W. Kasprzak: Method and apparatus for universal metallurgical simulation and analysis. US Patent 7,354,491, 8 April 2008.
135. F. Czerwinski: in *Magnesium Alloys: Properties in Solid and Liquid States*, F. Czerwinski, ed., Intech, Rijeka, 2014, pp. 131–70.
136. J. Russ and R. Dehoff: *Practical Stereology*, Springer, New York, 2000.
137. K. Carlson and C. Beckermann: *Int. J. Cast Met. Res.*, 2012, vol. 25, p. 75.
138. E. Tzimas and A. Zavaliangos: *J. Mater. Sci.*, 2000, vol. 35, pp. 5319–29.
139. E. Tzimas and A. Zavaliangos: *Mater. Manuf. Process.*, 1999, vol. 14, pp. 217–30.
140. Y. Wang, G. Liu, and Z. Fan: *Acta Mater.*, 2006, vol. 54, pp. 689–99.
141. F. Czerwinski, A. Zielinska-Lipiec, P. Pinet, and J. Overbeeke: *Acta Mater.*, 2001, vol. 49, pp. 1225–35.
142. F. Czerwinski: Near liquidus injection molding process. US Patent 7,255,151 B2, 14 Aug 2007.
143. F. Czerwinski: *Acta Mater.*, 2005, vol. 53, pp. 1973–84.
144. F. Czerwinski: *Scripta Mater.*, 2003, vol. 48, pp. 327–31.
145. R. Cahn: *Physical Metallurgy*, North Holland, Amsterdam, 1966.
146. T. Wolfsdorf-Brenner, P. Voorhees, and J. Sutliff: *J. Metall. Mater. Trans.*, 1999, vol. 30, p. 1955.
147. L. Ratke and P. Voorhees: *Growth and Coarsening*, Springer, Berlin, 2002.
148. I.M. Lifshitz and V. Slyozov: *J. Phys. Chem. Solids*, 1961, vol. 19, pp. 35–50.
149. C. Wagner: *Zeitung der Elektrochemie*, 1961, vol. 65, p. 581.
150. M. Marder: *Phys. Rev. A*, 1987, vol. 36, pp. 858–74.
151. D. Liu and H. Atkinson: *Trans. Nonferr. Met. Soc. China*, 2010, vol. 20, pp. 1672–76.
152. H. Atkinson and D. Liu: *Mater. Sci. Eng. A*, 2008, vol. 496, pp. 439–46.
153. J. Jiang, Y. Wang, and S. Luo: *Mater. Charact.*, 2007, vol. 58, pp. 190–96.
154. S. Kleiner, O. Beffort, and P. Uggowitzer: *Scripta Mater.*, 2004, vol. 51, pp. 405–10.
155. G. Yan, S. Zhao, S. Ma, and H. Shou: *Mater. Charact.*, 2012, vol. 69, pp. 45–51.
156. X. Hu, Q. Zhu, H. Lu, F. Zhang, D. Li, and S. Midson: *J. Alloys Compd*, 2015, vol. 649, pp. 204–10.
157. M. Emamy, A. Razaghian, and M. Karshenas: *Mater. Des.*, 2013, vol. 46, pp. 824–31.
158. A. Haghparast, M. Nourimotlagh, and M. Alipour: *Mater. Charact.*, 2012, vol. 71, pp. 6–18.
159. Q. Tang, H. Sun, M. Zhou, and G. Quan: *Metals*, 2017, vol. 7, p. 416.
160. Z. Ji, M. Hu, S. Sugiyama, and J. Yanagimoto: *Mater. Charact.*, 2008, vol. 59, pp. 905–11.
161. U. Curle: *SP 17 Proc. 6th Decenn. Int. Conf. Solidif. Process.*, Old Windsor, July 2017.
162. B. Binesh and M. Aghaie-Khafri: *Mater. Res. Express*, 2017, vol. 4, p. 096502.
163. W. Loue and M. Suery: *Mater. Sci. Eng. A*, 1995, vol. 203, pp. 1–13.
164. C. Bale: *Calphad*, 2016, vol. 54, pp. 35–53.
165. T. Chen, Y. Hao, and J. Sun: *Mater. Sci. Eng. A*, 2002, vol. 337, pp. 73–81.
166. S. Zhang, T. Chen, Y. Ma, Y. Li, and Y. Hao: *Appl. Mech. Mater.*, 2014, vols. 446–447, pp. 55–61.
167. S. Terzi, L. Salvo, M. Suery, and E. Boller: *Scripta Mater.*, 2009, vol. 60, pp. 671–74.
168. V. Kilicli, N. Akar, M. Erdogan, and K. Kocatepe: *J. Sci. Technol. Union Mech. Eng.*, 2012, vol. 9, pp. 25–28.
169. M. Flemings: *Metall. Trans.*, 1974, vol. 5, pp. 2121–34.
170. A. Kazakov: *Adv. Mater. Process.*, 2000, vol. 157, pp. 31–34.
171. H. Atkinson, P. Kapranos, D. Liu, and D. Kirkwood: *Mater. Sci. Forum*, 2002, vols. 396–402, pp. 131–36.
172. Y. Wang, S. Zhao, and C. Zhang: *Mater. Trans.*, 2017, vol. 58, pp. 176–81.
173. M. Mohammed, M. Omar, J. Sayarif, Z. Sajuri, M. Salleh, and K. Alhawari: *Sci. World J.*, 2013, Article ID 828926, pp. 1–7.
174. M. Omar, A. Alfian, J. Syarif, and H. Atkinson: *J. Mater. Sci.*, 2011, vol. 46, pp. 7696–7705.
175. M. Mohammed, M. Omar, M. Salleh, and K. Alhawari: *Adv. Mater. Sci. Eng.*, 2013, pp. 1–8.
176. M. Mohammed, M. Omar, J. Syarif, Z. Sajuri, M. Salleh, and K. Alhawari: *Appl. Mech. Mater.*, 2013, vols. 465–466, pp. 829–33.
177. B. Binesh and M. Aghaie-Khafri: *Metals*, 2016, vol. 42. <https://doi.org/10.3390/met6030042>.

178. Y. Wang, S. Zhao, and X. Zhao: *MATEC Web Conf.*, D2ME, 2017, vol. 136, art. no. 01003. <https://doi.org/10.1051/mateconf/201713601003>.
179. Y. Sirong, L. Dongcheng, and N. Kim: *Mater. Sci. Eng. A*, 2006, vol. 420, pp. 165–70.
180. S. Numsarapatnuk and S. Chayong: *Songklanakarini J. Sci. Technol.*, 2013, vol. 35, pp. 569–77.
181. G. Ansel and J. McDonnals: Method of rolling magnesium base alloys. US Patent 2,294,648, 1 Sep 1942.
182. N. Stanford: *Mater. Sci. Eng. A*, 2010, vol. 527, pp. 2669–77.
183. S. Sandlöbes, M. Friák, S. Korte-Kerzel, Z. Pei, J. Neugebauer, and D. Raabe: *Sci. Rep.*, 2017, vol. 7, p. 10458.
184. D. Griffiths: *Mater. Sci. Technol.*, 2015, vol. 31, pp. 10–24.
185. F. Czerwinski: *Int. J. Powder Metall.*, 2005, vol. 41, pp. 64–70.
186. W. Misiolek, M. Haase, N. Khalifa, A. Tekkaya, and M. Kleiner: *CIRP Ann.*, 2012, vol. 61, pp. 239–42.
187. Z. Wang, Z. Ji, L. Sun, and H. Xu: *Trans. Nonferr. Met. Soc. China*, 2010, vol. 20, p. s744.
188. P. Li, T. Chen, and H. Qin: *Mater. Des.*, 2016, vol. 112, pp. 34–45.
189. Y. Cao, C. Guo, S. Zhu, N. Wei, R. Javed, and F. Jiang: *Mater. Sci. Eng. A*, 2015, vol. 637, pp. 235–42.
190. T. Chen, H. Qin, and X. Zhang: *J. Mater. Sci.*, 2018, vol. 53, pp. 2576–93.
191. A. Rassili and M. Robelet: in *Thixoforming Steel*, H. Atkinson and A. Rassili, eds., Shaker Verlag, Aachen, 2010, pp. 87–103.
192. A. Bolouri, Y. Jeon, and C. Kang: *Int. J. Adv. Manuf. Technol.*, 2014, vol. 70, pp. 2139–49.
193. J. Jiang, H. Atkinson, and Y. Wang: *J. Mater. Sci. Technol. (Shenyang, China)*, 2017, vol. 33, pp. 379–88.
194. Y. Birol: *Int. J. Mater. Res.*, 2007, vol. 98, pp. 54–59.
195. A. Bolouri, M. Shamiri, and E. Cheshmeh: *Trans. Nonferr. Met. Soc. China*, 2010, vol. 20, pp. 1663–71.
196. L. Rogal: *Mater. Sci. Eng. A*, 2018, vol. 709, pp. 139–51.
197. L. Wang, W. Jiang, T. Chen, Y. Feng, H. Zhou, S. Zhao, Z. Liang, and Y. Zhu: *Trans. Nonferr. Met. Soc. China*, 2012, vol. 22, pp. s435–44.
198. J. Valle, T. Perez-Prado, and J. Bartolome: *Mater. Trans.*, 2003, vol. 44, pp. 2625–30.
199. C. Zhang, S. Zhao, and G. Yan: *J. Eng. Manuf.*, 2018, vol. 232, pp. 487–98.
200. Y. Meng, S. Sugiyama, M. Soltanpour, and J. Yanagimoto: *J. Mater. Process. Technol.*, 2013, vol. 213, pp. 426–33.
201. L. Rogal and J. Dutkiewicz: *Metall. Mater. Trans. A*, 2012, vol. 43A, pp. 5009–18.
202. Y. Meng, S. Sugiyama, and J. Yanagimoto: *J. Mater. Process. Technol.*, 2014, vol. 214, pp. 87–96.
203. J. Jiang, Y. Wang, Z. Du, and S. Luo: *Trans. Nonferr. Met. Soc. China*, 2012, vol. 22, pp. 422–27.
204. J. Jiang and S. Luo: *Trans. Nonferr. Met. Soc. China*, 2007, vol. 17, pp. 46–50.
205. T. Chen, G. Lu, Y. Ma, Y. Li, and Y. Hao: *J. Alloys Compd.*, 2009, vol. 486, pp. 124–35.
206. J. Jufua, W. Ying, Q. Jianjun, D. Zhiminga, S. Yi, and L. Shoujing: *J. Alloys Compd.*, 2010, vol. 497, pp. 62–67.
207. T. Chen, L. Wang, J. Yang, and S. Lu: *Int. J. Adv. Manuf. Technol.*, 2017, vol. 90, pp. 1639–47.
208. Z. Huang, R. Chen, and E. Han: *Mater. Sci. Forum*, 2009, vols. 610–613, pp. 806–09.
209. Y. Xu, J. Jia, C. Chen, W. Liu, S. Luo, Y. Yang, and L. Hu: *Int. J. Adv. Manuf. Technol.*, 2017, vol. 93 (9–12), pp. 4317–28.
210. Z. Zhao, Q. Chen, Y. Wang, and D. Shu: *Trans. Nonferr. Met. Soc. China*, 2009, vol. 19, pp. 535–39.
211. A. Dodanegeh, M. Kazeminezhad, and H. Aashuri: *Int. J. Cast Met. Res.*, 2014, vol. 27, pp. 312–20.
212. H. Jiang, X. Li, A. Xiong, and M. Li: *J. Mater. Eng. Perform.*, 2003, vol. 12, pp. 249–53.
213. G. Hirt, R. Cremer, A. Winkelmann, T. Witulski, and M. Zillgen: *J. Mater. Process. Technol.*, 1994, vol. 45, pp. 359–64.
214. C. Lin, F. Hung, and T. Lui: *Aluminium Alloys—Recent Trends in Processing, Characterization, Mechanical Behavior and Applications*, Intech, Rijeka, 2017, pp. 279–312.
215. T. Kaneuchi, R. Shibata, and M. Ozaw: in *7th International Conference on Advanced Semi-solid Processing of Alloys and Composites*, Y. Tsutsui, M. Kiuchi, and K. Ichikawa, eds., September 2002, Tsukuba, Japan, National Institute of Advanced Industrial Science and Technology and Japan Society for Technology, Tsukuba, Japan, 2002.
216. N. Hamazoe, K. Ohwada, K. Sakamoto, and A. Suzuki: Method and apparatus for manufacturing semi-solidified metal. European Patent EP 1050353, 24 Nov 2004.
217. J. Yurko and R. Boni: *Metall. Ital.*, 2006, vol. 3, pp. 35–41.
218. J. Yurko: *Die Cast. Eng.*, 2004, vol. 48, pp. 50–52.
219. R. Busk: Method for making thixotropic materials. US Patent 4,694,882, 22 Sep 1987.
220. R. Busk: Method for making thixotropic materials. US Patent 4,694,881, 22 Sep 1987.
221. N. Bradley, R. Wieland, W. Schafer, and A. Niemi: Method and apparatus for the injection molding of metal alloys. US Patent 5,040,589, 20 Aug 1991.
222. D. Doutre, G. Hay, P. Wales, and J. Gabathuler: *Can. Metall. Q.*, 2004, vol. 43, pp. 265–72.
223. J. Langlais and A. Lemieux: *Solid State Phenom.*, 2006, vols. 472–477, pp. 116–17.
224. D. Doutre, G. Hay, and P. Wales: Semisolid concentration processing of metallic alloys. US Patent 6,428,636 B2, 6 Aug 2002.
225. K. Richard, I. Neill, and C. Rice: Semi-solid casting apparatus and method. Patent PCT/US1999/016560, 3 Feb 2000.
226. A. Leatham, A. Ogilvy, P. Chesney, and J. Wood: *Met. Mater.*, 1989, vol. 5, pp. 140–43.
227. A. Ogilvy: *Acta Metall.*, 1992, vol. 9, pp. 33–46.
228. A. Leatham and A. Ogilvy: Method of manufacture of a thixotropic deposit. US Patent 4,804,034, 14 Feb 1989.
229. L. Ivanchev, D. Wilkins, G. Govender, W. Du Preez, and R. Bea: *S. Afr. J. Sci.*, 2008, vol. 104, pp. 257–59.
230. Z. Fan, S. Ji, and G. Liu: *Mater. Sci. Forum*, 2005, vols. 488–489, pp. 405–12.
231. S. Ji, Z. Zhen, and Z. Fan: *Mater. Sci. Technol.*, 2005, vol. 21, pp. 1019–24.
232. K. Young and M. Gjestland: *IMA Automot. Semin.*, Livonia, USA, 1995, April.
233. R. O'Donnell: *Die Cast. Eng.*, 2005, vol. 49, pp. 50–54.
234. Q. Pan, D. Apelian, and P. Hogan: *Metall. Sci. Technol.*, 2006, vol. 24, pp. 9–18.
235. W. Bernard: The Continuous Rheoconversion Process: Scale-Up and Optimization. Thesis, Worcester Polytechnic Institute, Worcester, MA, 2006.
236. D. Browne, M. Hussey, A. Carr, and D. Brabazon: *Int. J. Cast Met. Res.*, 2003, vol. 16, pp. 418–26.
237. A. Carr, D. Brown, M. Hussey, N. Lumsden, and M. Scanlan: *Int. J. Cast Met. Res.*, 2007, vol. 20, pp. 325–32.
238. K. Symeonidis: The Controlled Diffusion Solidification Process: Fundamentals and Principles, Ph.D. Thesis, Worcester Polytechnic Institute, Worcester, MA, 2009.
239. K. Kaufmann and P. Uggowitzer: *Adv. Eng. Mater.*, 2001. [http://doi.org/10.1002/1527-2648\(200112\)3:12%3c963::aid-adem963%3e3.0.co;2-x](http://doi.org/10.1002/1527-2648(200112)3:12%3c963::aid-adem963%3e3.0.co;2-x).
240. *Diecasting Times*, 2002, August–September, pp. 20–22.
241. J. Jorstad, M. Thieman, R. Kamm, M. Loughman, and T. Woehlke: *AFS Trans.*, 2003, vol. 80, paper 03-162.
242. B. Xing, Y. Li, Y. Ma, and Y. Hao: *China Foundry*, 2011, vol. 8, pp. 121–26.
243. B. Xing, Y. Hao, Y. Li, Y. Ma, and T. Chen: *Trans. Nonferr. Met. Soc. China*, 2013, vol. 23, pp. 567–75.
244. J. Lee and S. Kim: *Mater. Sci. Eng. A*, 2007, vols. 449–451, pp. 680–83.
245. H. Gjestland and H. Westegen: Procedure for the production of thixotropic magnesium alloy. US Patent 5,501,748, 26 March 1996.
246. J. Wannasin, S. Junodom, T. Rattanochaikul, and M. Flemings: *Solid State Phenom.*, 2008, vols. 141–143, pp. 97–102.
247. Z. Yang, L. Zhou, and J. Dong: *Trans. Nonferr. Met. Soc. China*, 2010, vol. 20, pp. 1579–84.
248. L. Rogal: *Mater. Des.*, 2017, vol. 119, pp. 406–16.
249. M. Avedesian and H. Baker: *Magnesium and Magnesium Alloys*, ASM International, Materials Park, OH, 1999.
250. *Metals Handbook*, ASM International, Materials Park, OH, 1990, vol. 1.
251. H. Mohammadi and M. Ketabchi: *Iran. J. Mater. Sci. Eng.*, 2013, vol. 10, pp. 32–43.

252. R. Gupta, A. Sharma, and S. Kumar: *IJRSI*, 2014, vol. 1, pp. 21–24.
253. F. Czerwinski: *Proc. 8th Int. Conf. Semisolid Process. Alloys Compos.*, paper 222, Limassol, Cyprus, 2004.
254. H. Ahlborn, E. Hornbogen, and U. Koster: *J. Mater. Sci.*, 1969, vol. 4, pp. 944–50.
255. M. Vaseghia: *Procedia Mater. Sci.*, 2015, vol. 11, pp. 418–22.
256. T. Sakai, X. Yang, and H. Miura: *Mater. Sci. Eng. A*, 1997, vols. 234–236, pp. 857–60.
257. J. Wang: Doctoral Dissertation, Jilin University, Jilin, 2005.
258. A. Javaid, M. Kozdras, and F. Czerwinski: *Adv. Mater. Process.*, 2018, vol. 176, pp. 16–21.